1975

FINAL REPORT

ELASTIC STRESS ANALYSIS OF GENERAL PRISMATIC BEAMS

by

S. D. Leftwich
Graduate Assistant

and

F. W. Barton
Faculty Research Scientist

(The opinions, findings, and conclusions expressed in this report are those of the authors and not necessarily those of the sponsoring agencies.)

Virginia Highway & Transportation Research Council
(A Cooperative Organization Sponsored Jointly by the Virginia Department of Highways & Transportation and the University of Virginia)

In Cooperation with the U. S. Department of Transportation
Federal Highway Administration

Charlottesville, Virginia

November 1980
VHTRC 81-R26

1979

BRIDGE RESEARCH ADVISORY COMMITTEE

J. M. MCCABE, JR., Chairman, Asst. Bridge Engineer, VDH&T

F. L. BURROUGHS, Construction Engineer, VDH&T

C. L. CHAMBERS, Division Structural Engineer, FHWA

H. L. Kinnier, Consultant, VH&TRC

J. G. G. MCGEE, Construction Control Engineer, VDH&T

W. T. MCKEEL, JR., Highway Research Scientist, VH&TRC

M. F. MENEFEE, JR., Structural Steel Engineer, VDH&T

L. L. MISENHEIMER, District Bridge Engineer, VDH&T

R. H. MORECOCK, District Bridge Engineer, VDH&T

W. W. PAYNE, Professor of Civil Engineering, VPI & SU

F. L. PREWOZNIK, District Bridge Engineer, VDH&T

M. M. SPRINKEL, Highway Research Scientist, VH&TRC

F. G. SUTHERLAND, Bridge Engineer, VDH&T

D. A. TRAYNHAM, Prestressed Concrete Engineer, VDH&T

SUMMARY

This study developed a numerical methodology for the elastic stress analysis of general prismatic beams. The objective was to accurately determine stresses and displacements on a cross section of a beam where the stress resultants are prescribed. Applied loads may include axial force, bending moment, uniform (constant) torsion, constant (transverse) shear, and the rates of change of twisting moment, axial force, and shear. By assuming that the stresses and strains in a beam vary as a quadratic function of the longitudinal coordinate, the formulation expressed in terms of displacement functions was reduced from a three-dimensional analysis to a two-dimensional one. Numerical solutions were obtained using the finite element method of analysis. Numerical results were compared with exact and approximate solutions for selected cross sections. Several representative beams having cross sections commonly used in bridges were used to demonstrate the applicability of the method.

1973

1979

FINAL REPORT

ELASTIC STRESS ANALYSIS OF GENERAL PRISMATIC BEAMS

by

S. D. Leftwich
Graduate Assistant

and

F. W. Barton
Faculty Research Scientist

PROBLEM STATEMENT

In traditional bridge design, elementary beam theory has been sufficient to predict both the deformations and the normal stress distributions resulting from the bending moment carried by the girder. Using this elementary theory, it was appropriate to utilize the basic assumption of beam theory; namely, that cross sections of the beam remain plane after bending.

In the design of contemporary bridge structures, however, irregular cross sections and curved geometries are frequently encountered. In such cases, certain of the more traditional and approximate methods of analysis may be incapable of accurately predicting the stress distribution throughout the structure. In the presence of significant shear stresses, caused either by torsion or by transverse loading on the bridge, cross sections may not remain plane and the basic assumption of beam theory may lead to results seriously in error. For certain geometries, such as those found in thin walled sections utilized in many box girder bridges, it is not unusual for longitudinal restraint in the presence of nonuniform torsion to contribute significantly to the normal stresses and corresponding deformation.

The problem of reliably predicting both normal and shearing stresses in the cross section of bridge girders is not new. Extensive research has been conducted in the past decade, with emphasis on the determination of stress resultants such as bending moments, shearing forces, and torques at particular cross sections of the bridge girder, as well as the determination of detailed stress distributions throughout the cross section once these overall stress resultants have been determined.[1,2] Shearing stresses and the accompanying change in normal stress distribution due to restrained warping have been studied extensively for the case of torsional loads, and both approximate and more exact techniques for calculating such stresses have been developed.[3,4]

However, the complexity of the problem has made it impossible to completely determine the effects of all parameters. In particular, the effect of nonuniform shear on normal stresses and corresponding cross-sectional deformation cannot, at the present time, be reliably predicted. Nonuniform shear can occur either when the loading varies along the axis of the beam or when the warping of the cross section, caused by the shear at that location, is constrained by the end conditions or mechanical devices. Current practice calls for these effects to simply be neglected; however, preliminary consideration has indicated that, in certain cases of cross-sectional geometry, these effects may be significant.

There is, then, a need to study the effects of previously neglected parameters such as nonuniform shear on the deformation and stresses in beams whose geometries are such that these effects may produce significant changes in the usual bending stresses. The results from such a study would provide a more accurate procedure for the stress analysis of thin walled cross sections and, more importantly, would identify for bridge designers the relative importance of these parameters.

OBJECTIVES

The broad objective of this study was to develop a theoretical background, based on an exact elasticity formulation, and a subsequent numerical procedure for the general elastic stress analysis of straight beams of arbitrary cross section. Existing approximations permit the stress analysis of beams under certain loading conditions such as constant shear, uniform torsion, and nonuniform or restrained torsion.[2,3,4,5,6] Although the formulation is sufficiently general to include other types of loadings, the primary concern was the effect of nonuniform shear on the normal stress distribution over the cross section.

Specific objectives include the following:

1. To formulate, using elasticity theory, a theoretical basis for subsequent numerical approximations with consideration given to all loading parameters, i.e., constant shear, uniform and nonuniform torsion, etc., but with primary emphasis given to the effects of nonuniform shear.

2. To develop a general numerical method for the stress analysis of beams of arbitrary cross section that would include consideration of nonuniform shear and restrained warping, with emphasis given only to a finite element procedure to arrive at numerical approximations.

3. To demonstrate this method by calculating the normal and shearing stresses for beams having certain representative cross sections such as rectangular, circular, angle, channel, and box sections.

4. To compare the stress results for certain cross sections with either the exact solutions or previously determined approximate solutions. The exact solution for nonuniform shear may be obtained for the rectangular and circular sections.

5. To evaluate the effects of nonuniform shear on stresses and the stress distributions over the cross sections.

SCOPE

In the study, consideration was limited to prismatic beams having straight axes and subjected to arbitrary loadings. The material of the beam was assumed to be homogeneous, although the method can be extended to consider composite action. Numerical results were limited to typical cross-sectional geometries such as open or closed box members currently used in the design of girder highway bridges. The feasibility of extending the procedure developed for the straight beam analysis to include curved beams was determined.

DEVELOPMENT OF THEORY

In the development of the theoretical background for the elastic stress analysis, it was assumed that the bending moment, shearing force, torque, bimoment, or other appropriate stress resultants at any specified location along the axis of the beam are known.

Consider a beam of arbitrary cross section, loaded uniformly along its axis with either body forces or surface tractions. The forces which determine the magnitude of the uniform load may be of any distribution either on the periphery or in the cross section of the beam. Figure 1 depicts the coordinate system used with the x and y axes in the plane of the cross section of the beam and with the origin at the centroid. Figure 2 depicts the forces or surface tractions which may be associated with the uniformly loaded beam.

1983

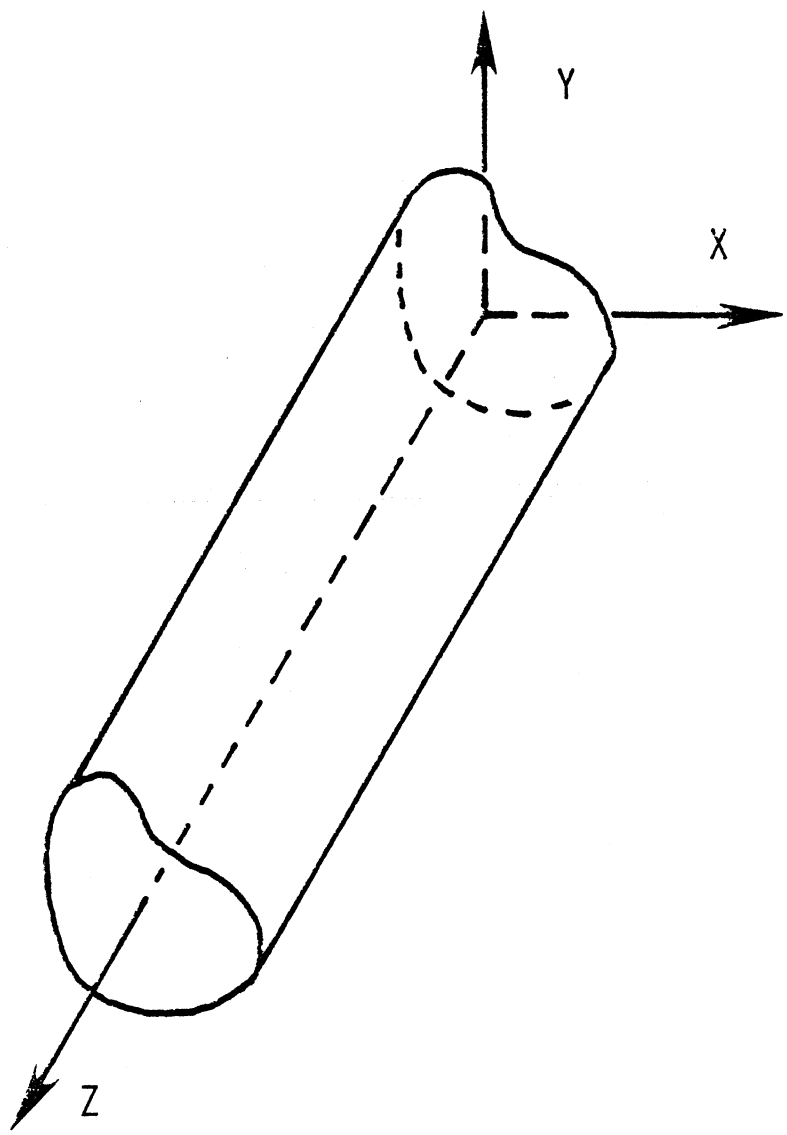

Figure 1. Coordinate system.

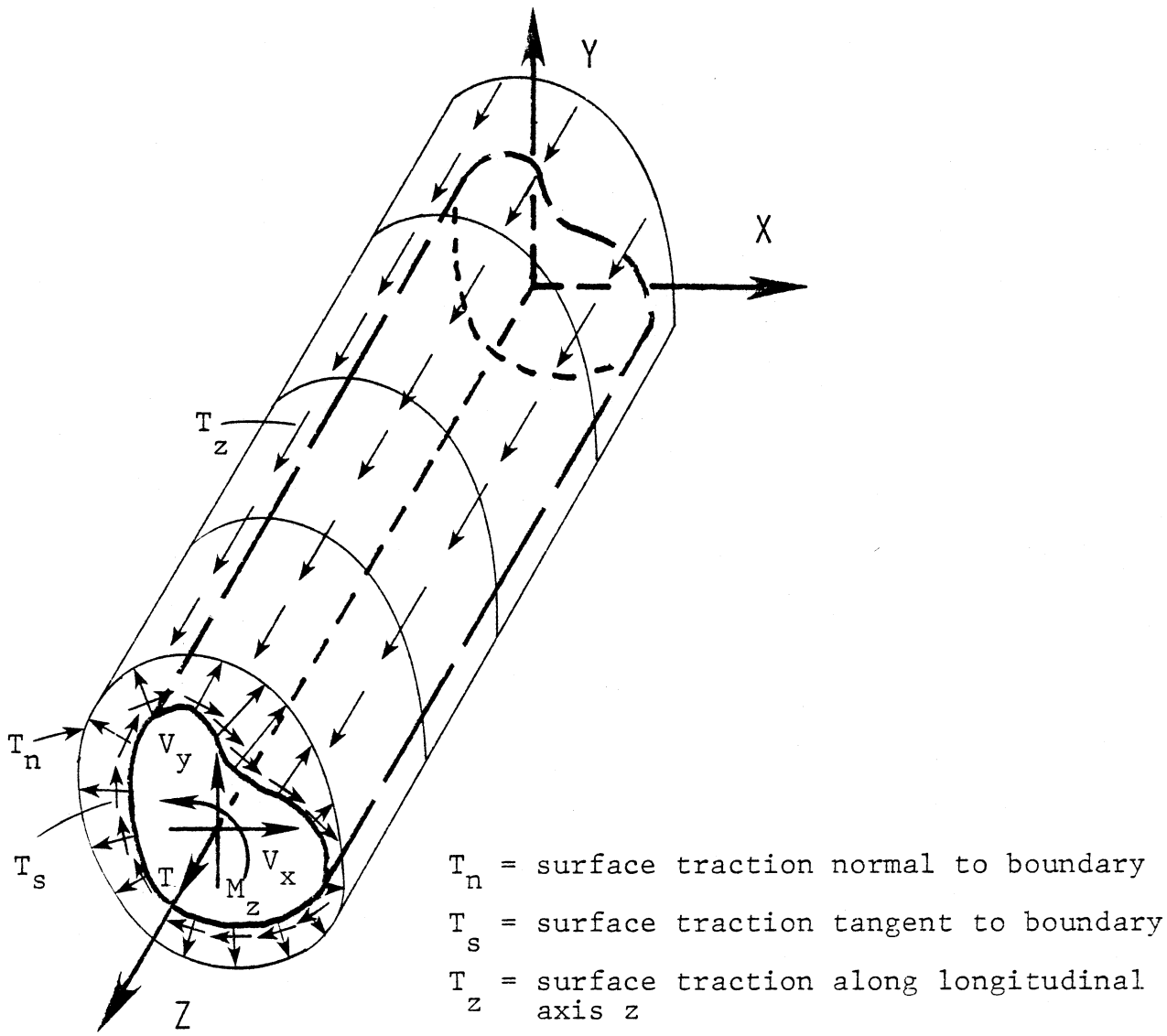

Figure 2. Forces on the uniformly loaded beam.

The following assumptions are made:

1. The material is isotropic, linear, homogeneous, and continuous.

2. The z axis is the centroidal axis, but the x and y axes are not necessarily principal axes.

3. The beam is prismatic and the distribution of the uniform load over the cross section may be arbitrary. This work covers the cases of a uniform distribution of twisting couple and longitudinal force. Any resultant force or couple at any end of the beam is also considered.

4. The stresses and strains may be expressed as a quadratic function of the longitudinal coordinate z.

Assumption (4) reduces the problem from a three-dimensional one to a two-dimensional or cross-sectional analysis and allows the stresses and strains to depend only upon the internal forces, couples, and other appropriate stress resultants at that cross section.

Consistent with assumption (4), the stresses are assumed to be of the form:

$$\sigma_x = \sigma_x^{(2)}(x,y)z^2 + \sigma_x^{(1)}(x,y)z + \sigma_x^{(0)}(x,y) \tag{1a}$$

$$\sigma_y = \sigma_y^{(2)}(x,y)z^2 + \sigma_y^{(1)}(x,y)z + \sigma_y^{(0)}(x,y) \tag{1b}$$

$$\sigma_z = \sigma_z^{(2)}(x,y)z^2 + \sigma_z^{(1)}(x,y)z + \sigma_z^{(0)}(x,y) \tag{1c}$$

$$\tau_{xy} = \tau_{xy}^{(2)}(x,y)z^2 + \tau_{xy}^{(1)}(x,y)z + \tau_{xy}^{(0)}(x,y) \tag{1d}$$

$$\tau_{xz} = \tau_{xz}^{(2)}(x,y)z^2 + \tau_{xz}^{(1)}(x,y)z + \tau_{xz}^{(0)}(x,y) \tag{1e}$$

$$\tau_{yz} = \tau_{yz}^{(2)}(x,y)z^2 + \tau_{yz}^{(1)}(x,y)z + \tau_{yz}^{(0)}(x,y). \tag{1f}$$

Similarly, the strains are assumed to be given by

$$\varepsilon_x = \varepsilon_x^{(2)}(x,y)z^2 + \varepsilon_x^{(1)}(x,y)z + \varepsilon_x^{(0)}(x,y) \tag{2a}$$

$$\varepsilon_y = \varepsilon_y^{(2)}(x,y)z^2 + \varepsilon_y^{(1)}(x,y)z + \varepsilon_y^{(0)}(x,y) \tag{2b}$$

$$\varepsilon_z = \varepsilon_z^{(2)}(x,y)z^2 + \varepsilon_z^{(1)}(x,y)z + \varepsilon_z^{(0)}(x,y) \tag{2c}$$

$$\gamma_{xy} = \gamma_{xy}^{(2)}(x,y)z^2 + \gamma_{xy}^{(1)}(x,y)z + \gamma_{xy}^{(0)}(x,y) \tag{2d}$$

$$\gamma_{xz} = \gamma_{xz}^{(2)}(x,y)z^2 + \gamma_{xz}^{(1)}(x,y)z + \gamma_{xz}^{(0)}(x,y) \tag{2e}$$

$$\gamma_{yz} = \gamma_{yz}^{(2)}(x,y)z^2 + \gamma_{yz}^{(1)}(x,y)z + \gamma_{yz}^{(0)}(x,y). \tag{2f}$$

In the equilibrium and compatibility equations, the boundary conditions, and the stress-strain laws, the terms of the second, first, and zero degrees in z may be considered separately.

The first step is to substitute eqq. 1a-2f into the appropriate equilibrium and compatibility equations. Enforcing the boundary conditions, and taking terms that contain only z^2, the following relations are derived:

$$\sigma_x^{(2)} = \sigma_y^{(2)} = \tau_{xy}^{(2)} = \gamma_{xy}^{(2)} = 0 \tag{3a}$$

$$\varepsilon_x^{(2)} = \varepsilon_y^{(2)} = -\mu\varepsilon_z^{(2)} = \mu(-\varepsilon_2 + a_2 x + b_2 y) \tag{3b}$$

$$\varepsilon_z^{(2)} \quad \varepsilon_2 - a_2 x - b_2 y \tag{3c}$$

$$\sigma_z^{(2)} = E\varepsilon_z^{(2)} \tag{3d}$$

$$\tau_{xz}^{(2)} = G\gamma_{xz}^{(2)} = G\theta_2\left(\frac{\partial\phi}{\partial x} - y\right) \tag{3e}$$

$$\tau_{yz}^{(2)} = G\gamma_{yz}^{(2)} = G\theta_2\left(\frac{\partial\phi}{\partial y} + x\right), \tag{3f}$$

where $\phi(x,y)$ is St. Venant's torsion function, and θ_2, ε_2, a_2, and b_2 are constants with

$$\nabla^2\phi(x,y) = 0 \qquad \text{in } R \tag{3g}$$

$$\frac{\partial\phi}{\partial n} = y\ell - xm \qquad \text{on } C \tag{3h}$$

In a similar fashion, if those terms containing only z are collected, the following expressions are derived:

$$\theta_2 = \gamma_{xz}^{(2)} = \tau_{xz}^{(2)} = \gamma_{yz}^{(2)} = \tau_{yz}^{(2)} = \varepsilon_2$$
$$= \sigma_x^{(1)} = \sigma_y^{(1)} = \gamma_{xy}^{(1)} = \tau_{xy}^{(1)} = 0 \tag{4a}$$

$$\varepsilon_z^{(1)} = \varepsilon_1 - a_1x - b_1y \tag{4b}$$

$$\varepsilon_x^{(1)} = \varepsilon_y^{(1)} = -\mu\varepsilon_z^{(1)} = -\mu(\varepsilon_1 - a_1x - b_1y) \tag{4c}$$

$$\sigma_z^{(1)} = E\varepsilon_z^{(1)} = E(\varepsilon_1 - a_1x - b_1y) \tag{4d}$$

$$\gamma_{yz}^{(1)} = \theta_1\left(\frac{\partial\phi}{\partial y} + x\right) + 2a_2\left[\frac{\partial\psi_1}{\partial y} + \mu xy\right]$$
$$+ 2b_2\left[\frac{\partial\psi_2}{\partial y} + \frac{1}{2}\mu(y^2 - x^2)\right] \tag{4e}$$

$$\gamma_{xz}^{(1)} = \theta_1\left(\frac{\partial\phi}{\partial x} - y\right) + 2a_2\left[\frac{\partial\psi_1}{\partial x} + \frac{1}{2}\mu(x^2 - y^2)\right]$$
$$+ 2b_2\left[\frac{\partial\psi_2}{\partial x} + \mu xy\right] \tag{4f}$$

$$\tau_{yz}^{(1)} = G\gamma_{yz}^{(1)} \tag{4g}$$

$$\tau_{xz}^{(1)} = G\gamma_{xz}^{(1)}, \tag{4h}$$

where $\phi(x,y)$ is the torsion function, $\psi_1(x,y)$ and $\psi_2(x,y)$ are the warping functions in the x-z and y-z planes, respectively, due to shearing deformation, ε_1, a_1, b_1, and θ_1 are constants, and with

$$\nabla^2\phi\ (x,y) = 0 \tag{4i}$$

$$\nabla^2\psi_1(x,y) = 2x \tag{4j}$$

$$\nabla^2\psi_2(x,y) = 2y \tag{4k}$$

and

$$\frac{\partial\phi}{\partial n} = \ell y - mx \tag{4l}$$

$$\frac{\partial\psi_1}{\partial n} = -\ell\frac{1}{2}\mu(x^2 - y^2) - m\mu xy \tag{4m}$$

$$\frac{\partial\psi_2}{\partial n} = -\ell\mu xy - m\frac{1}{2}\mu(y^2 - x^2). \tag{4n}$$

Finally, by selecting terms independent of z, the following expressions are derived:

$$\gamma_{yz}^{(0)} = \theta_0\left(\frac{\partial\overline{\phi}}{\partial y} + x\right) + a_1\left[\frac{\partial\overline{\psi}_1}{\partial y} + \mu xy\right] + b_1\left[\frac{\partial\overline{\psi}_2}{\partial y} + \frac{1}{2}\mu(y^2 - x^2)\right] \tag{5a}$$

$$\gamma_{xz}^{(0)} = \theta_0\left(\frac{\partial\overline{\phi}}{\partial x} - y\right) + a_1\left[\frac{\partial\overline{\psi}_1}{\partial x} + \frac{1}{2}\mu(x^2 - y^2)\right] + b_1\left[\frac{\partial\overline{\psi}_2}{\partial x} + \mu xy\right] \tag{5b}$$

$$\varepsilon_z^{(0)} = \varepsilon_0 - a_0 x - b_0 y + \theta_1\phi(x,y) + 2a_2\psi_2(x,y) + 2b_2\psi_2(x,y) \tag{5c}$$

$$\varepsilon_1 = -\frac{1}{EA}\left[\int_C T_z ds + \iint \overline{Z}dxdy\right] \tag{5d}$$

$$\sigma_x^{(0)} = (\lambda + 2G)\varepsilon_x^{(0)} + \lambda\varepsilon_y^{(0)} + \lambda\varepsilon_z^{(0)} \tag{5e}$$

$$\sigma_y^{(0)} = (\lambda + 2G)\varepsilon_y^{(0)} + \lambda\varepsilon_x^{(0)} + \lambda\varepsilon_z^{(0)} \tag{5f}$$

$$\tau_{yz}^{(0)} = G\gamma_{yz}^{(0)} \tag{5g}$$

$$\tau_{xz}^{(0)} = G\gamma_{xz}^{0} \tag{5h}$$

$$\tau_{xy}^{(0)} = G\gamma_{xy}^{(0)} \tag{5i}$$

$$\varepsilon_x^{(0)} = \frac{\partial u^0}{\partial x} \tag{5j}$$

$$\varepsilon_y^{(0)} = \frac{\partial v^0}{\partial y} \tag{5k}$$

$$\gamma_{xy}^{(0)} = \frac{\partial u^0}{\partial y} + \frac{\partial v^0}{\partial x} \tag{5l}$$

$$\sigma_z^{(0)} = E\varepsilon_z^{(0)} + \mu(\sigma_x^{(0)} + \sigma_y^{(0)}) \tag{5m}$$

$$\nabla^2\overline{\phi} = 0 \tag{5n}$$

$$\nabla^2\overline{\psi}_1 = 2x \tag{5o}$$

$$\nabla^2\overline{\psi}_2 = 2y - \frac{1}{Gb_1}(E\varepsilon_1 + \overline{Z}) \tag{5p}$$

and

$$\frac{\partial\overline{\phi}}{\partial n} = \ell y - mx \tag{5q}$$

$$\frac{\partial\overline{\psi}_1}{\partial n} = -\ell\frac{1}{2}\mu(x^2 - y^2) - m\mu xy \tag{5r}$$

$$\frac{\partial\overline{\psi}_2}{\partial n} = -\ell\mu xy - m\frac{1}{2}\mu(y^2 - x^2) + \frac{T_z}{b_1 G} \tag{5s}$$

$$\overline{\phi}(x,y) = \phi(x,y) \tag{5t}$$

$$\overline{\psi}_1(x,y) = \psi_1(x,y), \tag{5u}$$

where θ_0, ε_0, a_0, and b_0 are constants.

If there is no distributed longitudinal force,

$$\overline{\psi}_2(x,y) = \psi_2(x,y). \tag{5v}$$

Using eqq. 1a-1f, 2a-2f, 3a-3f, 4a-4h, and 5a-5m, the final complete expressions for stresses and strains are as follows:

$$\varepsilon_x = \mu[(a_1 z + a_2 z^2)x + (b_1 z + b_2 z^2)y] - \mu\varepsilon_1 z + \varepsilon_x^{(0)} \tag{6a}$$

$$\varepsilon_y = \mu[(a_1 z + a_2 z^2)x + (b_1 z + b_2 z^2)y] - \mu\varepsilon_1 z + \varepsilon_y^{(0)} \tag{6b}$$

$$\varepsilon_z = \varepsilon_0 + \varepsilon_1 z - (a_0 + a_1 z + a_2 z^2)x - (b_0 + b_1 z + b_2 z^2)y + \theta_1\phi(x,y) + 2a_2\psi_1(x,y) + 2b_2\psi_2(x,y) \tag{6c}$$

$$\gamma_{xy} = \frac{\partial u^0}{\partial y} + \frac{\partial v^0}{\partial x} \tag{6d}$$

$$\gamma_{xz} = \mu[(a_1 + 2a_2 z)\tfrac{1}{2}(x^2 - y^2) + (b_1 + 2b_2 z)xy] + z[\theta_1(\frac{\partial\phi}{\partial x} - y) + 2a_2\frac{\partial\psi_1}{\partial x} + 2b_2\frac{\partial\psi_2}{\partial x}] + \theta_0(\frac{\partial\phi}{\partial x} - y) + a_1\frac{\partial\psi_1}{\partial x} + b_2\frac{\partial\overline{\psi}_2}{\partial x} \tag{6e}$$

$$\gamma_{yz} = \mu[(a_1 + 2a_2 z)xy + (b_1 + 2b_2 z)\tfrac{1}{2}(y^2 - x^2)] + z[\theta_1(\frac{\partial\phi}{\partial y} + x) + 2a_2\frac{\partial\psi_1}{\partial y} + 2b_2\frac{\partial\overline{\psi}_2}{\partial y}] + \theta_0(\frac{\partial\phi}{\partial y} + x) + a_1\frac{\partial\psi_1}{\partial y} + b_1\frac{\partial\overline{\psi}_2}{\partial y} \tag{6f}$$

$$\tau_{xy} = G\gamma_{xy} \tag{6g}$$

$$\tau_{xz} = G\gamma_{xz} \tag{6h}$$

$$\tau_{yz} = G\gamma_{yz} \tag{6i}$$

$$\sigma_x = (\lambda + 2G)\varepsilon_x^{(0)} + \lambda\varepsilon_y^{(0)} + \lambda\varepsilon_z^{(0)} \tag{6j}$$

$$\sigma_y = (\lambda + 2G)\varepsilon_y^{(0)} + \lambda\varepsilon_x^{(0)} + \lambda\varepsilon_z^{(0)} \tag{6k}$$

$$\sigma_z = E\varepsilon_z + \mu(\sigma_x + \sigma_y) \tag{6l}$$

$$\varepsilon_x^{(0)} = \frac{\partial u^0}{\partial x} \tag{6m}$$

$$\varepsilon_y^{(0)} = \frac{\partial v^0}{\partial y} \tag{6n}$$

$$\varepsilon_z^{(0)} = \varepsilon_0 - a_0 x - b_0 y + \theta_1\phi(x,y) + 2a_2\psi_1(x,y) + 2b_2\psi_2(x,y), \tag{6o}$$

where ε_0, ε_1, a_0, a_1, a_2, b_0, b_1, b_0, θ_0, and θ_1 are constants.

The evaluation of the constants in terms of applied loading and boundary conditions, and the interpretation of these constants, are derived elsewhere.(7)

DEVELOPMENT OF THE FINITE ELEMENT METHODOLOGY

Finite Element Theory

In this section, a procedure using the finite element method for approximately solving the equations developed in the previous section is presented.

The unknown functions to be determined using the finite element method are the warping functions $\phi(x,y)$, $\psi_1(x,y)$, $\psi_2(x,y)$, and $\psi_3(x,y)$ and the displacement functions $u^0(x,y)$ and $v^0(x,y.)$ An alternate way of representing the equations and boundary conditions governing these functions is to find their equivalent variational forms which, when minimized with respect to the unknown functions, will yield the governing differential equations and boundary conditions. These functionals, which are derived in reference (7), are designated I_ϕ, I_{ψ_1}, I_{ψ_2}, I_{ψ_3}, and I_0.

The finite element solution is obtained by varying the nodal values of the unknown variables so as to minimize the equivalent variational functional. Thus, setting the partial derivatives of the functional with respect to each of the unknown nodal variables equal to zero produces a set of algebraic equations. These equations can then be solved for the nodal values of the variables.

For the uniformly loaded beam, the cross section is approximated by a system of arbitrarily shaped triangular elements. The unknown variables are assumed to vary linearly within each element Figure 3 depicts a typical finite element idealization of a beam cross section and Figure 4 represents a typical m^{th} element with its nodes numbered as shown in its local numbering system.

By letting $\gamma(x,y)$ represent any one of the unknown variables, $\phi(x,y)$, $\psi_1(x,y)$, $\psi_2(x,y)$, $\psi_3(x,y)$, $u^0(x,y)$, or $v^0(x,y)$, the values of the unknown function at the nodes 1, 2, and 3 are denoted respectively by $\gamma_1{}^m$, $\gamma_2{}^m$, and $\gamma_3{}^m$.

The unknown variable may be expressed as a linear function within element m as

$$\gamma^m(x,y) = C_1^m + C_2^m x + C_3^m y \,, \qquad (7)$$

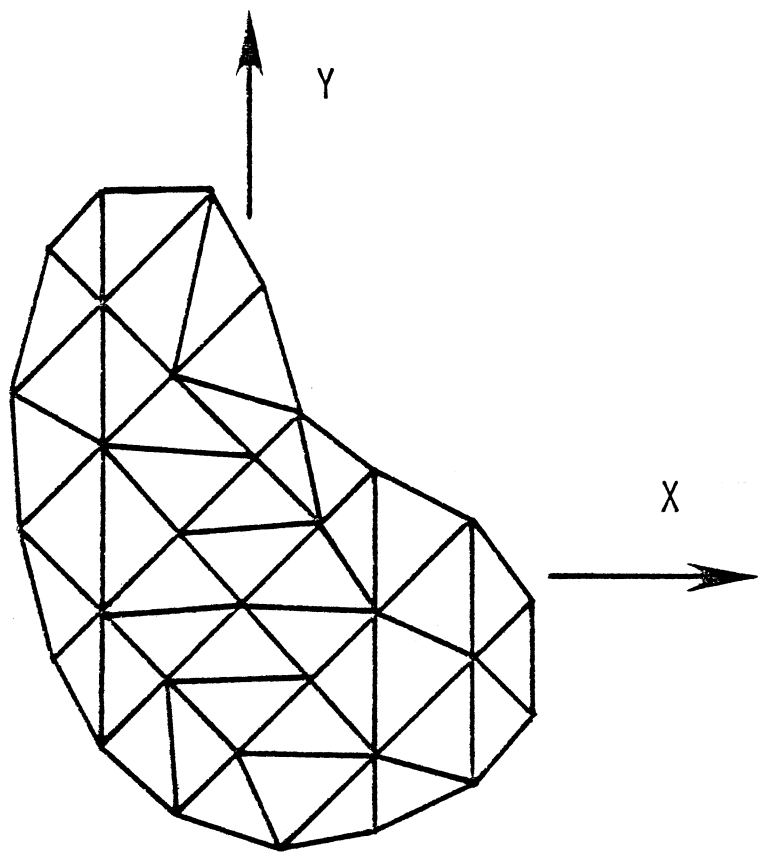

Figure 3. Finite element idealization of the beam cross section.

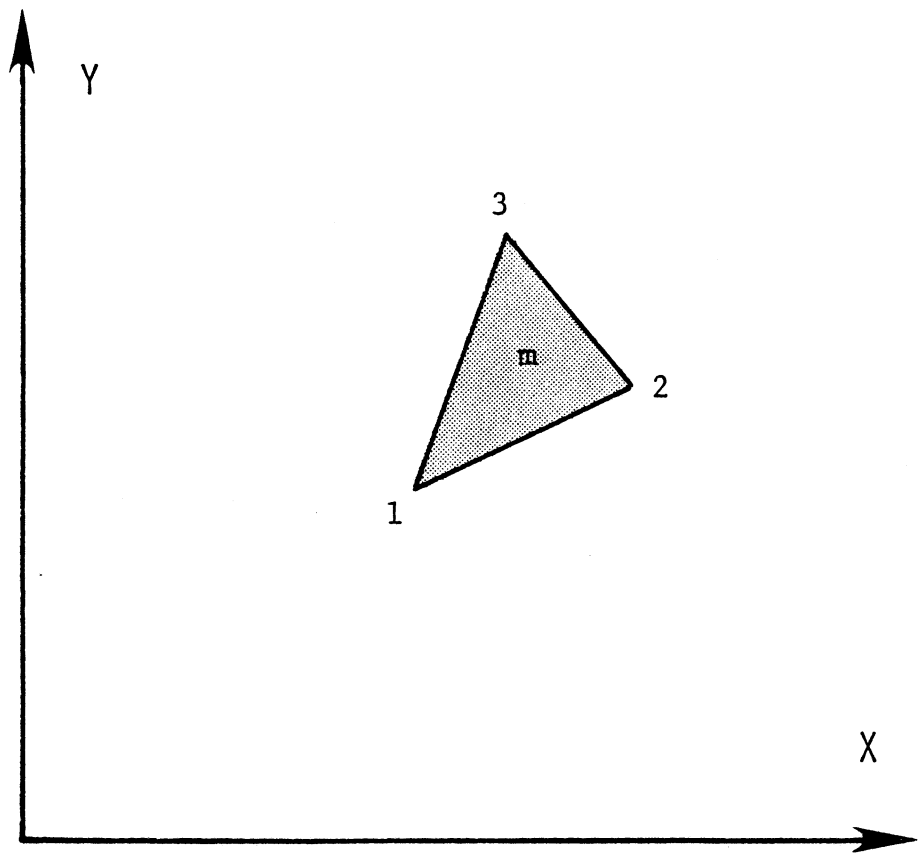

Figure 4. Typical triangular element.

where the constants C_1^m, C_2^m, and C_3^m can be determined in terms of the values of γ at the node points. These can be written in a simplified form using the summation convention as

$$C_i^m = T_{ij}^m \gamma_j^m \qquad j = 1,2,3, \qquad (8)$$

where a repeated subscript implies summation. In eq. (8),

$$T_{ij}^m = \frac{1}{2A^m} \begin{bmatrix} x_2y_3 - x_3y_2 & x_3y_1 - x_1y_3 & x_1y_2 - x_2y_1 \\ y_2 - y_3 & y_3 - y_1 & y_1 - y_2 \\ x_3 - x_2 & x_1 - x_3 & x_2 - x_1 \end{bmatrix}, \qquad (9)$$

and A^m = the area of element m.

Using eq. (8) and utilizing the summation convention, eq. (7) can be written in terms of the values of the unknown variable at the nodes of the element as

$$\gamma^m(x,y) = C_i^m X_i = T_{ij}^m \gamma_j^m X_i \qquad j = 1,2,3, \qquad (10)$$

where

$$X_i = [1 \ x \ y]. \qquad (11)$$

The derivatives of $\gamma(x,y)$ with respect to x and y may also be expressed in terms of the values of the unknown variable at the nodes of the element as

1994

$$\frac{\partial \gamma^m(x,y)}{\partial x} = T^m_{2j}\gamma^m_j \qquad j = 1,2,3 \qquad (12)$$

$$\frac{\partial \gamma^m(x,y)}{\partial y} = T^m_{3j}\gamma^m_j \qquad j = 1,2,3. \qquad (13)$$

For area integrations of a triangular element, let

$$X_r = [1 \;\; x \;\; y \;\; x^2 \;\; y^2] \qquad r = 1,2,3,4,5 \qquad (14)$$

$$I^m_{rs} = \iint_{A^m} X_r X_s \, dx\, dy = \langle X_r \;\; X_s \rangle \quad r, s = 1,2,3,4,5 \qquad (15)$$

$$I^m_{rs} = \begin{bmatrix} A^m & A^m\bar{x} & A^m\bar{y} & I^m_{yy} & I^m_{xx} \\ A^m\bar{x} & I^m_{yy} & I^m_{xy} & \langle x^3\rangle & \langle xy^2\rangle \\ A^m\bar{y} & I^m_{xy} & I^m_{xx} & \langle yx^2\rangle & \langle y^3\rangle \\ I^m_{yy} & \langle x^3\rangle & \langle x^2y\rangle & \langle x^4\rangle & \langle x^2y^2\rangle \\ I^m_{xx} & \langle y^2x\rangle & \langle y^3\rangle & \langle y^2x^2\rangle & \langle y^4\rangle \end{bmatrix}, \qquad (16)$$

and for line integrations, let

$$L_{ij} = \int_{S^m} X_i X_j \, ds \qquad i, j = 1,2,3, \qquad (17)$$

where X_i or X_j are given by eq. (11).

Warping Function Formulations

Warping Function $\phi(x,y)$

The energy functional to be minimized is

$$I_\phi = \frac{1}{2}\iint[(\frac{\partial\phi}{\partial x} - y)^2 + (\frac{\partial\phi}{\partial y} + x)^2]dxdy. \tag{18}$$

Using the notation as given by eqq. (10)-(13), eq. (18) may be expressed by

$$I_\phi = \sum_{m=1}^{M} \frac{1}{2} \iint_{A^m}[(T_{2j}^{n}\ \phi_j^m - y)^2 + (T_{3j}^{m}\ \phi_j^m + x)^2]dxdy, \tag{19}$$

where M = the total number of elements in the cross section.

Following the usual Ritz procedure, the minimization of the functional with respect to the unknown warping function ϕ_n leads to the following system of equations.

$$\sum_{m=1}^{Q} B_k \phi_k^m = \sum_{m=1}^{Q} C_n \qquad n = 1,2,3,\ldots L \quad k = 1,2,3, \tag{20a}$$

where

$$B_k = I_{11}^m\ [T_{2k}^m T_{2n}^m + T_{3k}^m T_{3n}^m] \tag{20b}$$

$$C_n = T_{2n}^m T_{13}^m - T_{3n}^m I_{12}^m \tag{20c}$$

$T_{in}^m = T_{ij}^m$, j = 1,2, or 3, the node number in element m which corresponds to node n, (20d)

Q is the number of elements which surround node n, L is the total number of node points defining the shape of the cross section, and I^m_{ij} is given by eq. (16).

Eq. (20a) can be solved for the values of the warping function ϕ at the node points.

This formulation for the torsional warping function $\phi(x,y)$ is identical to that given previously by Herrman[6] and by Pilkey.[8]

Warping Function $\psi_1(x,y)$

The energy functional to be minimized is

$$I_{\psi_1} = \frac{1}{2}\iint\{[\frac{\partial\psi_1}{\partial x} + \frac{1}{2}\mu(x^2 - y^2)]^2 + [\frac{\partial\psi_1}{\partial y} + \mu xy]^2$$

$$+ 4(1+\mu)\ x\psi_1(x,y)\}dxdy. \qquad (21)$$

Using the notation as given by eqq. (10)-(13), eq. (21) may be expressed by

$$I_{\psi_1} = \sum_{m=1}^{M} \frac{1}{2}\iint_{A^m}\{[T_{2j}^{m}\ \psi_{1j}^{m} + \frac{1}{2}\mu(x^2 - y^2)]^2$$

$$+ [T_{3j}^{m}\ \psi_{1j}^{m} + \mu xy]^2 + 4(1 + \mu)X_2X_iT_{ij}^{m}\psi_{1j}^{m}\}dxdy, \qquad (22)$$

where M = the total number of elements in the cross section.

Minimizing the energy of the system with respect to the unknown warping function ψ_{1n} yields:

$$\sum_{m=1}^{Q} S_{nj}^{m}\psi_{1j} = \sum_{m=1}^{Q} R_n \qquad n = 1,2,3,\ldots L \quad j = 1,2,3, \qquad (23a)$$

where

$$S_{nj} = [T_{2j}^{m} T_{2n}^{m} + T_{3j}^{m} T_{3n}^{m}] I_{1j}^{m} \tag{23b}$$

$$R_{n} = -\frac{1}{2}\mu(I_{22}^{m} - I_{33}^{m})T_{2n}^{m} - \mu I_{23}^{m} T_{3n}^{m} - 2(1 + \mu) I_{2i}^{m} T_{in}^{m} \tag{23c}$$

$T_{in}^{m} = T_{ij}^{m}$, $j = 1,2,$ or 3, the node number in element m which corresponds to node n, (23d)

Q is the number of elements which surround node n, L is the total number of node points, and I_{ij}^{m} is given by eq. (16).

Eq. (23a) may be solved for the values of the warping function ψ_1 at the node points.

Warping Function $\psi_2(x,y)$

The energy functional to be minimized is given by

$$I_{\psi_2} = \frac{1}{2}\iint\{[\frac{\partial\psi_2}{\partial x} + \mu xy]^2 + [\frac{\partial\psi_2}{\partial y} + \frac{1}{2}\mu(y^2 - x^2)]^2 + 4(1 + \mu)y\psi_2(x,y)\, dxdy, \tag{24}$$

which may be alternately expressed as

$$I_{\psi_2} = \sum_{m=1}^{M} \frac{1}{2}\iint_{A^m}\{[T_{2j}^{m}\, \psi_{2j}^{m} + \mu xy]^2 + [T_{3j}^{m}\, \psi_{2j}^{m} + \frac{1}{2}\mu(y^2 - x^2)]^2 + 4(1 + \mu)X_3 X_i T_{ij}^{m}\, \psi_{2j}^{m}\} dxdy, \tag{25}$$

where M = the total number of elements in the cross section.

Again, minimizing the energy of the system leads to the following set of linear equations.

$$\sum_{m=1}^{Q} \bar{S}_{nj} \psi_{2j}^{m} = \sum_{m=1}^{Q} \bar{R}_n \qquad n = 1,2,3,\ldots L \quad j = 1,2,3, \tag{26a}$$

where

$$\bar{S}_{nj} = [T_{2j}^{m} T_{2n}^{m} + T_{3j}^{m} T_{3n}^{m}] I_{11}^{m} \tag{26b}$$

$$\bar{R}_n = -\mu I_{23}^{m} T_{2n}^{m} - \frac{1}{2}\mu(I_{33}^{m} - I_{22}^{m}) T_{3n}^{m} - 2(1+\mu) I_{3i}^{m} T_{in}^{m} \tag{26c}$$

$T_{in}^{m} = T_{ij}^{m}$, j = 1,2, or 3, the node number in element m which corresponds to node n, (26d)

Q is the number of elements which surround node n, L is the total number of node points, and I_{ij}^{m} is given by eq. (16)

Eq. (26a) may be solved for the values of the warping function ψ_2 at the node points.

Warping Function $\psi_3(x,y)$

The energy functional to be minimized is given by

$$I_{\psi_3} = \frac{1}{2}\iint\{[\frac{\partial\psi_3}{\partial x} + \mu b_1 xy]^2 + [\frac{\partial\psi_3}{\partial y} + \frac{1}{2}\mu(y^2 - x^2)b_1]^2 + 4(1+\mu)b_1 y\psi_3(x,y) - \frac{2}{G}(E\varepsilon_1 + \bar{Z})\psi_3(x,y)\, dxdy - \int_c \frac{T_z}{G}\psi_3(x,y)\, ds, \tag{27}$$

which may be written as

$$I_{\psi_3} = \sum_{m=1}^{M} \frac{1}{2}\iint_{A^m} \{ [T_{2j}^m \psi_{3j}^m + b_1 xy]^2 + [T_{3j}^m \psi_{3j}^m + \frac{1}{2}\mu b_1 (y^2 - x^2)]^2$$

$$+ 4(1 + \mu) b_1 X_3 X_i \; T_{ij}^m \psi_{3j}^m - \frac{2}{G}(E\varepsilon_1 + \bar{Z}) X_i T_{ij}^m \psi_{3j}^m \} dxdy$$

$$- \sum_{m=1}^{M1} \frac{T_z}{G} X_i T_{ij}^m \; \psi_{3j}^m ds, \qquad (28)$$

where M = the total number of elements in the cross section and M1 = the total number of elements forming the boundary of the cross section.

Minimizing the energy of the system leads to the following set of linear equations.

$$\sum_{m=1}^{Q} \tilde{S}_{nj}^m \; \psi_{3j}^m = \sum_{m=1}^{Q} \tilde{R}_n \qquad \begin{array}{l} n = 1,2,3,\ldots L \\ J = 1,2,3, \end{array} \qquad (29a)$$

where

$$\tilde{S}_{nj} = [T_{2j}^m \; T_{2n}^m + T_{3j}^m \; T_{3n}^m] I_{11}^m - \mu b_1 I_{23}^m \; T_{2n}^m$$

$$- \frac{1}{2}\mu b_1 (I_{33}^m - I_{22}^m) T_{3n}^m \qquad (29b)$$

$$\tilde{R}_n = -2(1+\mu)b_1 I_{3i}^{m} T_{in}^{m} + \frac{1}{G}(E\varepsilon_1 + \bar{Z}) I_{1i}^{m} T_{in}^{m} + \frac{T_z}{G} L_{1j} T_{iN}^{m} \tag{29c}$$

$T_{in}^{m} = T_{ij}^{m}$, $j = 1,2,$ or 3, the node number in element m which corresponds to node n, (29d)

Q is the number of elements which surround node n, L is the total number of node points, I_{ij}^{m} is given by eq. (16), and L_{ij} is given by eq. (17). Only when node n lies on the boundary and T_z is specified as a nontrivial value will the last integral in eq. (29c) contribute to eq. (29a).

Displacement Functions $u^0(x,y)$ and $v^0(x,y)$

The energy functional to be minimized is given by

$$I_0 = \iint\{\tfrac{1}{2}[\lambda(\varepsilon_x^{(0)} + \varepsilon_y^{(0)} + \varepsilon_z^{(0)})^2 + 2G(\varepsilon_x^{(0)2} + \varepsilon_y^{(0)2}) + G\gamma_{xy}^{(0)2}] - (\tau_{xz}^{(1)} + \bar{X})u^0 - (\tau_{yz}^{(1)} + \bar{Y})v^0\}dxdy - \int_c (T_x u^0 + T_y v^0)ds, \tag{30}$$

where

$$\varepsilon_x^{(0)} = \frac{\partial u^0}{\partial x} \tag{31a}$$

$$\varepsilon_y^{(0)} = \frac{\partial v^0}{\partial y} \tag{31b}$$

$$\gamma_{xy}^{(0)} = \frac{\partial u^0}{\partial y} + \frac{\partial v^0}{\partial x}. \tag{31c}$$

Using eqq. (31a)-(31c), the notation as given by eqq. (10)-(13), and dropping the superscript ^{0} on $u^0(x,y)$ and $v^0(x,y)$, eq. (30) may be expressed by

$$I_0 = \sum_{m=1}^{M} \iint_{A^m} \{\tfrac{1}{2}\lambda(T_{2j}^{m}\, u_j^m + T_{3j}^{m}\, v_j^m + \varepsilon_z^{(0)})^2$$

$$+ G[(T_{2j}^{m}\, u_j^m)^2 + (T_{3j}^{m}\, v_j^m)^2] + \tfrac{1}{2}G[T_{3j}^{m}\, u_j^m + T_{2j}^{m}\, v_j^m]^2$$

$$- (\tau_{xz}^{(1)} + \bar{X})X_i T_{ij}^{m}\, u_j^m - (\tau_{yz}^{(1)} + \bar{Y})X_i T_{ij}^{m}\, v_j^m\}dxdy$$

$$- \sum_{m=1}^{M1} \int_{S^m} [T_x X_i T_{ij}^{m}\, u_j^m + T_y X_i T_{ij}^{m}\, v_j^m]ds, \qquad (32)$$

where M = the total number of elements in the cross section and M1 = the total number of elements forming the boundary of the cross section.

By minimizing the energy of the system with respect to the unknown displacement functions u_m and v_m, the following set of linear equations are derived for u and v, respectively.

$$\sum_{m=1}^{Q} \iint_{A^m} \{\lambda(T_{2j}^{m}\, u_j^m + T_{3j}^{m}\, v_j^m + \varepsilon_z^{(0)})T_{2n}^{m}$$

$$+ 2G\, T_{2j}^{m}\, T_{2n}^{m}\, u_j^m + G(T_{3j}^{m}\, u_j^m + T_{2j}^{m}\, v_j^m)T_{3n}^{m}$$

$$- (\tau_{xz}^{(1)} + \bar{X})X_i T_{in}^{m}\}\, dxdy - \sum_{m=1}^{Q} \int_{S^m} T_x X_i T_{in}^{m}\, ds = 0$$

(33a)

$$\sum_{m=1}^{Q} \iint_{A^m} \{\lambda(T_{2j}^m u_j^m + T_{3j}^m v_j^m + \varepsilon_z^{(0)})T_{3n}^m$$

$$+ 2G\, T_{3j}^m T_{3n}^m v_j^m + G(T_{3j}^m u_j^m + T_{2j}^m v_j^m)T_{2n}^m$$

$$- (\tau_{yz}^{(1)} + \bar{Y})X_i T_{in}^m\} dxdy - \sum_{m=1}^{Q} \int_{S^m} T_y X_i T_{in}^m \, ds = 0. \qquad (33b)$$

Performing the above element integrations and using eqq. (16) and (17), eqq. (33a)-(33b) yield the following system of 2L linear simultaneous equations.

$$\sum_{m=1}^{Q} [K]^m \{\Delta\}^m = \sum_{m=1}^{Q} \{P\}^m \qquad \begin{array}{l} n = 1,2,3 \ldots L \\ j = 1,2,3, \end{array} \qquad (34a)$$

where

$$\{\Delta\}^m = \begin{Bmatrix} u_j^m \\ v_j^m \end{Bmatrix} \qquad j = 1,2,3, \qquad (34b)$$

$$\{P\}^m = \begin{Bmatrix} P_1^m \\ P_2^m \end{Bmatrix} \qquad (34c)$$

$$[K]^m = \begin{bmatrix} k_{11}^m & k_{12}^m \\ k_{21}^m & k_{22}^m \end{bmatrix} I_{11}^m, \qquad (34d)$$

where

$$k_{11}^m = (\lambda + 2G)T_{2j}^m T_{2n}^m + G(T_{3j}^m T_{3n}^m) \tag{34e}$$

$$k_{12}^m = \lambda T_{3j}^m T_{2n}^m + G T_{2j}^m T_{3n}^m \tag{34f}$$

$$k_{21}^m = \lambda T_{3n}^m T_{2j}^m + G T_{2n}^m T_{3j}^m \tag{34g}$$

$$k_{22}^m = (\lambda + 2G)T_{3j}^m T_{3n}^m + G T_{2j}^m T_{2n}^m \tag{34h}$$

$$P_1^m = -\lambda T_{2n}^m \iint_{A^m} \varepsilon_z^{(0)} dxdy + T_{in}^m \iint_{A^m} \tau_{xz}^{(1)} X_i dxdy$$

$$+ \bar{X} I_{1i}^m T_{in}^m + T_x T_{in}^m L_{1i} \tag{34i}$$

$$P_2^m = -\lambda T_{3n}^m \iint_{A^m} \varepsilon_z^{(0)} dxdy$$

$$+ T_{in}^m \iint_{A^m} \tau_{yz}^{(1)} X_i dxdy + \bar{Y} I_{1i}^m T_{in}^m + T_y T_{in}^m L_{1i} \tag{34j}$$

$T_{in}^m = T_{ij}^m$, j = 1, 2, or 3, the node number in element m which corresponds to node n, (34k)

Q is the number of elements which surround node n, L is the total number of node points, I_{ij}^m is given by eq. (16), and L_{ij} is given by eq. (17).

Boundary Conditions

The stiffness matrices for the warping functions and displacement functions given by eqq. (20a), (23a), (26a), (29a), and (34a) are singular and the corresponding equations cannot be solved uniquely. To overcome this difficulty, certain boundary conditions must be applied by selecting an arbitrary node and specifying the

values of $\phi(x,y)$, $\psi_1(x,y)$, $\psi_2(x,y)$, and $\psi_3(x,y)$ at that node. Since the stresses from these functions will not be affected by the specified values of the warping functions, the values of $\phi(x,y) = \psi_1(x,y) = \psi_2(x,y) = \psi_3(x,y) = 0$ at the selected node are acceptable.

For the displacement functions $u^0(x,y)$ and $v^0(x,y)$, it is necessary to zero three displacements to prevent rigid body motion. Since the cross section, theoretically, is in equilibrium under the forces given by eq. (34c), the stresses derived from the displacement functions will not be affected by the constraints chosen.

The displacement functions $u^0(x,y)$ and $v^0(x,y)$ will provide a mapping of the cross-sectional distortion created by the applied forces on the cross section. Therefore, in order to obtain a sketch of the cross-sectional distortion, it is convenient to constrain an interior element near the shear center so the boundary of the cross section is the least affected. If the shear center is outside the cross section, an interior element near the centroid may be constrained.

APPLICATIONS AND NUMERICAL EXAMPLES

The stresses considered in this study include those due to constant torsion, direct shear, bending moment, axial force, nonuniform torsion, and nonuniform shear. The stresses due to nonuniform torsion and shear require the determination of warping functions which are determined approximately using a finite element analysis.

A finite element computer program has been prepared to determine these warping functions. Input loading parameters include the magnitudes of the axial force, bending moment, twisting moment, and the rates of change of twisting moment and shear. Rates of change of twisting moment or shear may be input either as body forces or as surface tractions in which case the surface traction connectivity on the outer boundary of the cross section must be specified.

In this section, several examples are presented to demonstrate the applicability of this methodology. Comparisons of the finite element solutions with the exact or approximate solutions for certain cross sections will also be given to demonstrate the accuracy of the former. Emphasis is given to those stresses resulting from nonuniform shear.

This computer program was developed as a research tool and is not suitable for general use at this time. Those interested in the details of the program may contact the authors.

Rectangular Section

Consider a homogeneous beam of a rectangular solid cross section in which the material has a modulus of elasticity of 199,950 MPa (29,000,000 psi) and a Poisson's ratio of 0.27. The beam is subjected to a uniform load of 17.5 kN/m (100 lb./in.) uniformly distributed on the upper surface of the beam as a surface traction of 68.95 kPa (10 psi). The dimensions and the finite element model of the beam cross section, including the loading, are depicted in Figure 5. The resultant shearing force on the cross section to be analyzed is 4,448 N (1,000 lb.) in the positive y direction.

An approximate generalized plane stress solution to this problem has been presented by Love[9] in which the average of the normal stress in the x direction is taken to be zero. Comparisons of stresses from the generalized plane stress solution and the finite element model are given in Table 1. For a constant value of y, the average of the stresses in a row of elements is tabulated as the finite element solution. These stresses are graphically depicted in Figures 6-8, with small triangles denoting the approximate average finite element solutions. The comparisons of stresses as depicted in the table and graphs show good agreement for both the shearing stress and the normal stresses.

To determine the u and v displacements, boundary conditions must be imposed as discussed earlier. In this example, the centroid was fixed against displacement and rotation. Figure 9 depicts the cross-sectional distortion of the beam cross section due to three loading conditions. The values of the nodal displacements may be found from formulae derived by several authors[9,10,11,12] and have the magnitudes of $\pm 88.68 \times 10^{-6}$ mm ($\pm 3.49138 \times 10^{-6}$in.) and $\pm 66.51 \times 10^{-6}$mm ($\pm 2.61853 \times 10^{-6}$ in.) for u and v, respectively. Displacements from the finite element formulation give corresponding values of $\pm 86,89 \times 10^{-6}$mm ($\pm 3.42099 \times 10^{-6}$ in.) and $\pm 66.09 \times 10^{-6}$mm ($\pm 2.60178 \times 10^{-6}$ in.), which differ by only 2.0% and 0.6% from the exact solutions. Thus, it may be concluded that this methodology quite accurately predicts the cross-sectional distortion of the rectangular section under pure bending.

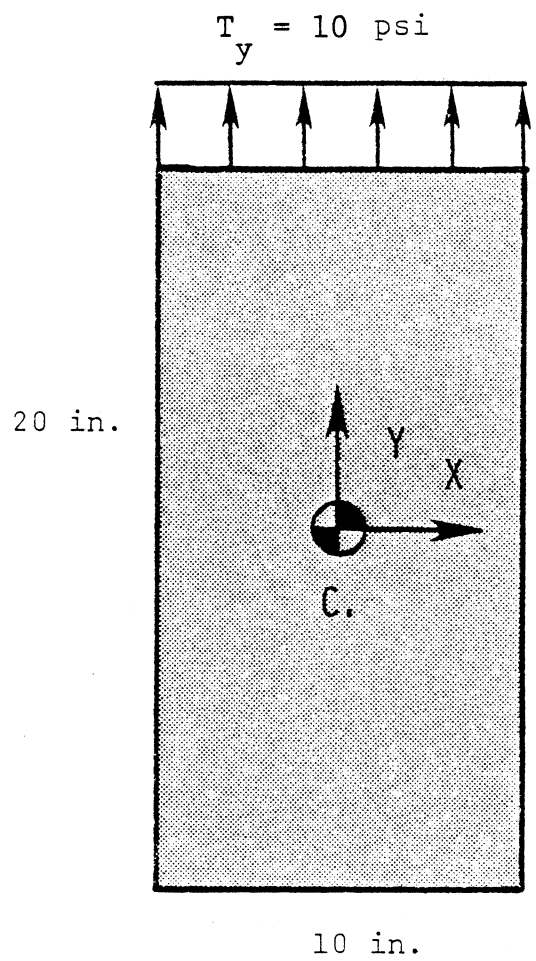

1 in. = 25.4 mm

1 psi = 6.89 kPa

Figure 5. Solid rectangular section subjected to a uniformly distributed surface traction of 10 psi.

TABLE 1

Comparison of Stresses For a Rectangular Section

Y Distance	τ_{yz}		σ_y		σ_z	
	G. P. S.*	F. E.**	G. P. S.*	F. E.**	G. P. S.*	F. E.**
8.5714	1.9898	1.9428	9.8542	9.7200	0.5772	0.6324
5.7143	5.0510	5.0041	8.8193	8.7297	-0.7813	-0.7663
2.8571	6.8878	6.8408	7.0845	7.0399	-0.7405	-0.7355
0.0	7.5000	7.4531	5.0000	5.0000	0.0	-0.0003
-2.8571	6.8878	6.8408	2.9155	2.9603	0.7405	0.7350
-5.7143	5.0510	5.0041	1.1808	1.2704	0.7813	0.7678
-8.5714	1.9898	1.9428	0.1458	0.2801	-0.5772	-0.6240

* Generalized plane stress solutions from Love in psi
** Averaged finite element solutions in psi

1 in. = 25.4 mm
1 psi = 6.89 kPa

2007

2003

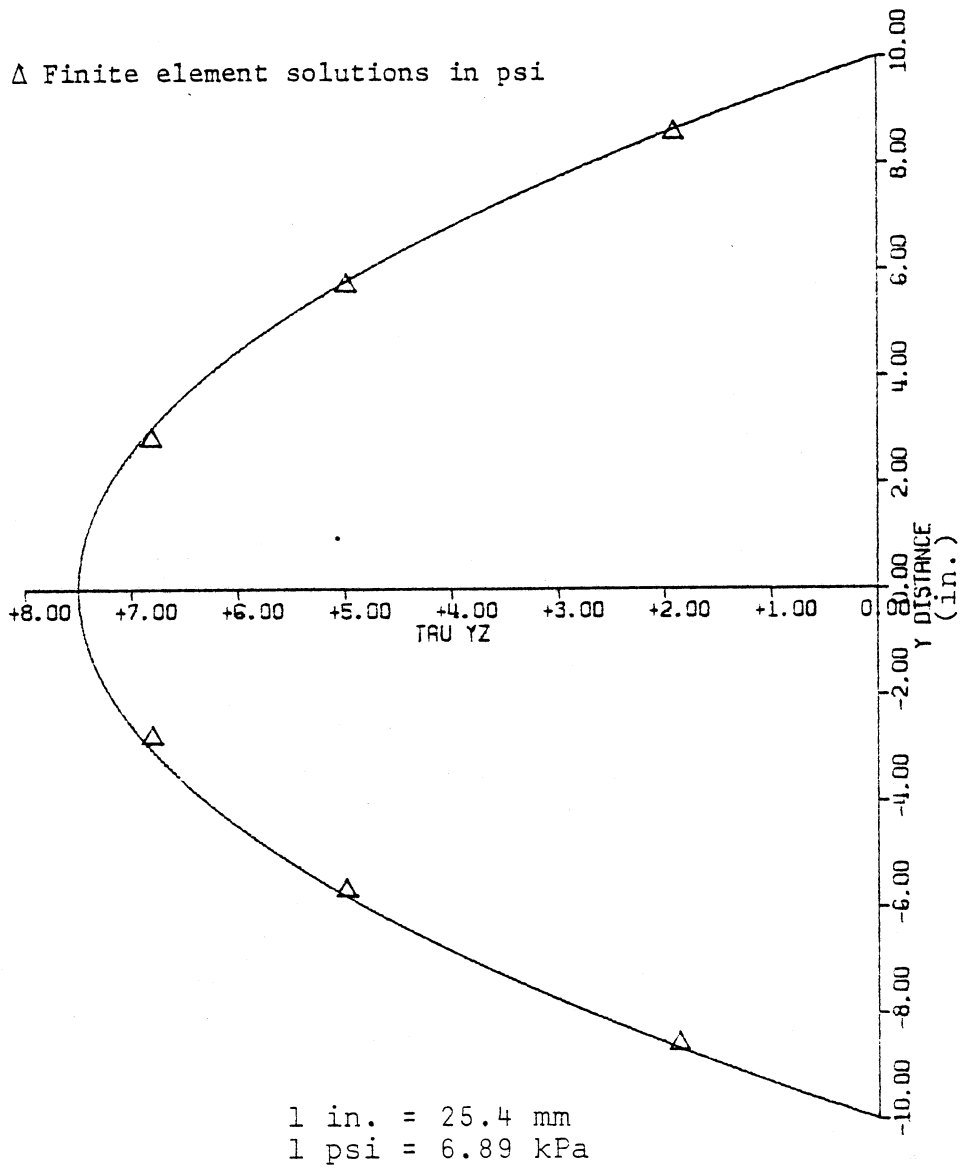

Figure 6. Shear stress (τ_{yz}) distribution in a rectangular section.

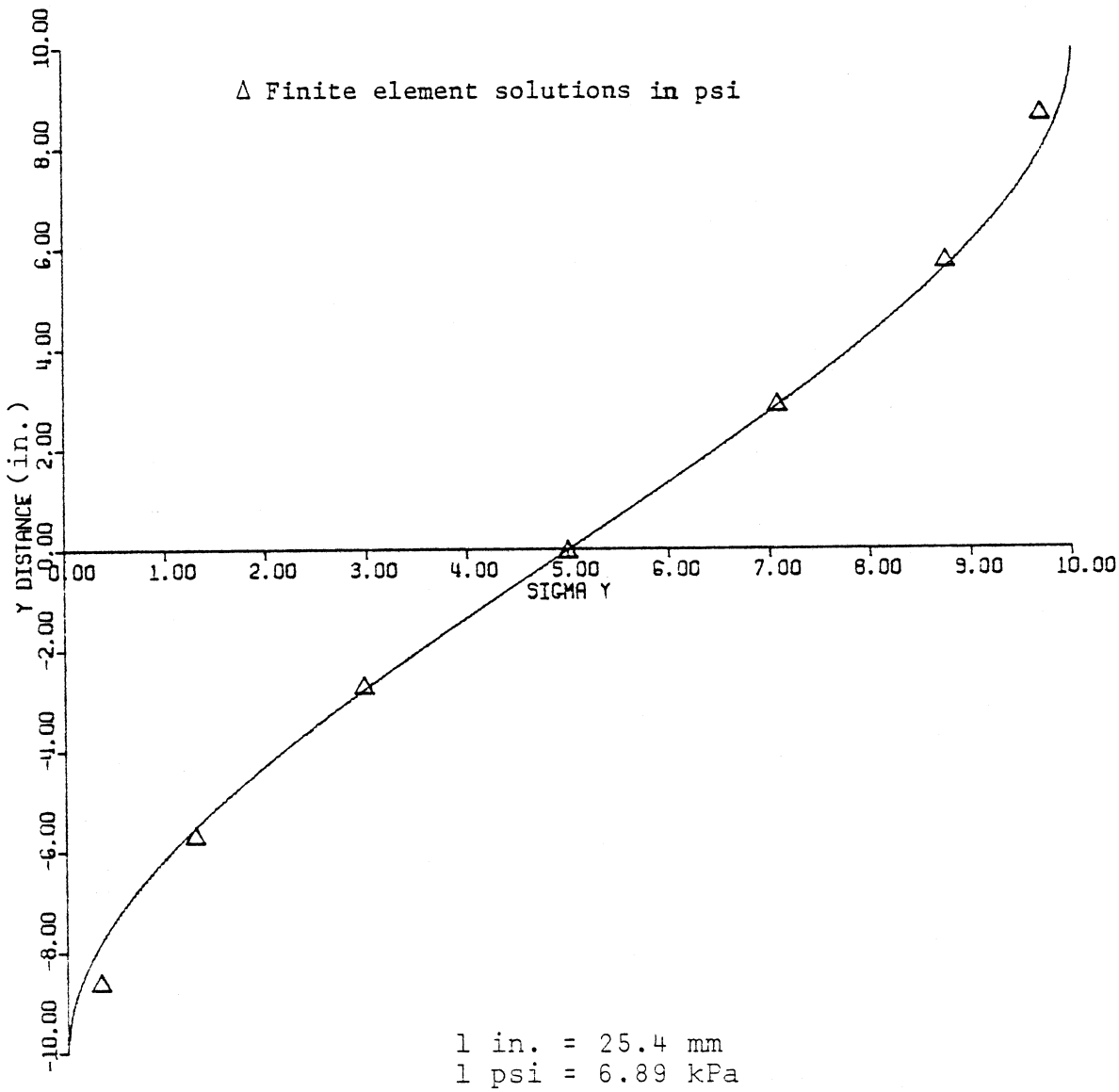

Figure 7. Normal stress (σ_y) distribution in a rectangular section.

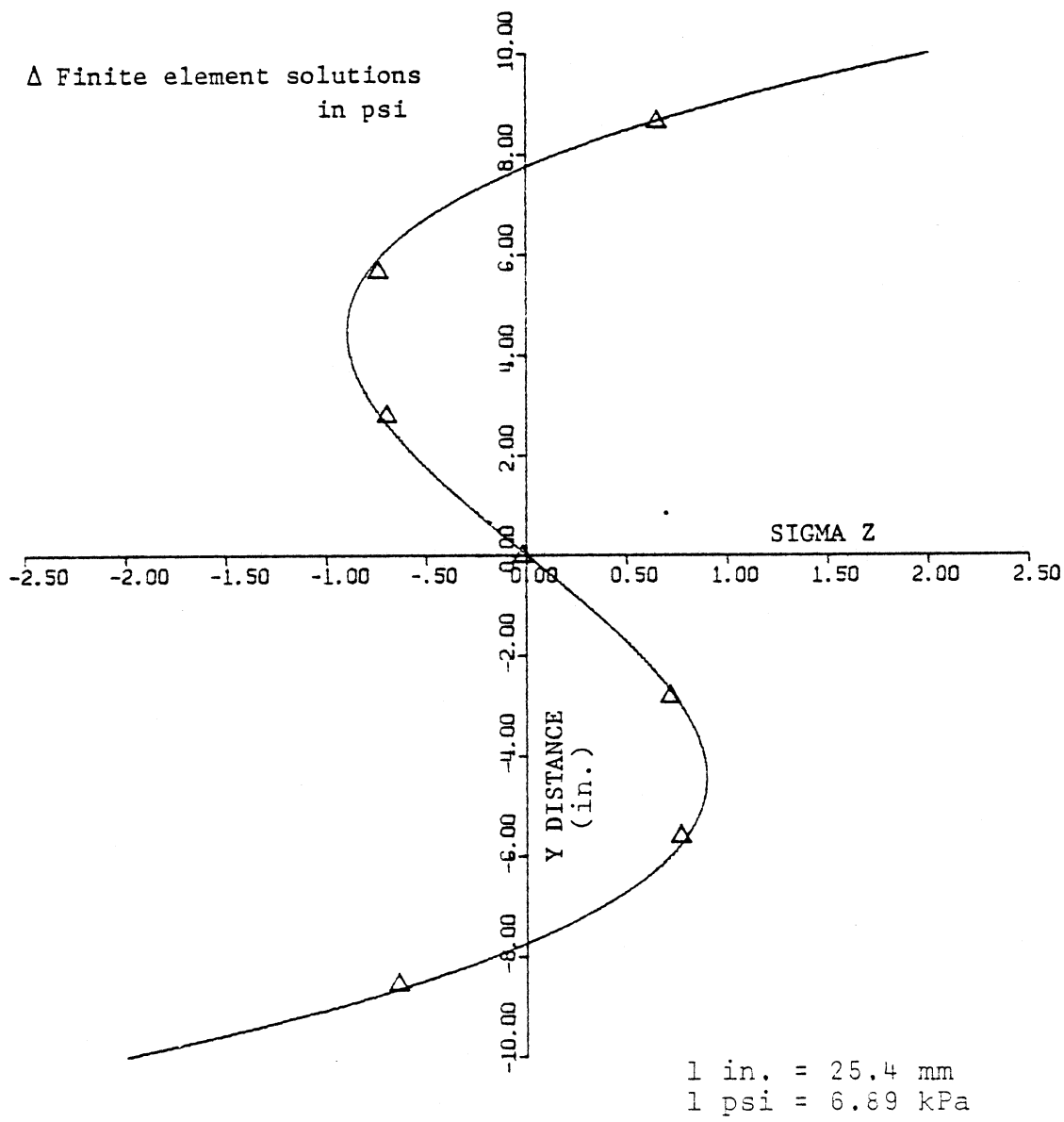

Figure 8. Normal stress (σ_z) distribution in a rectangular section.

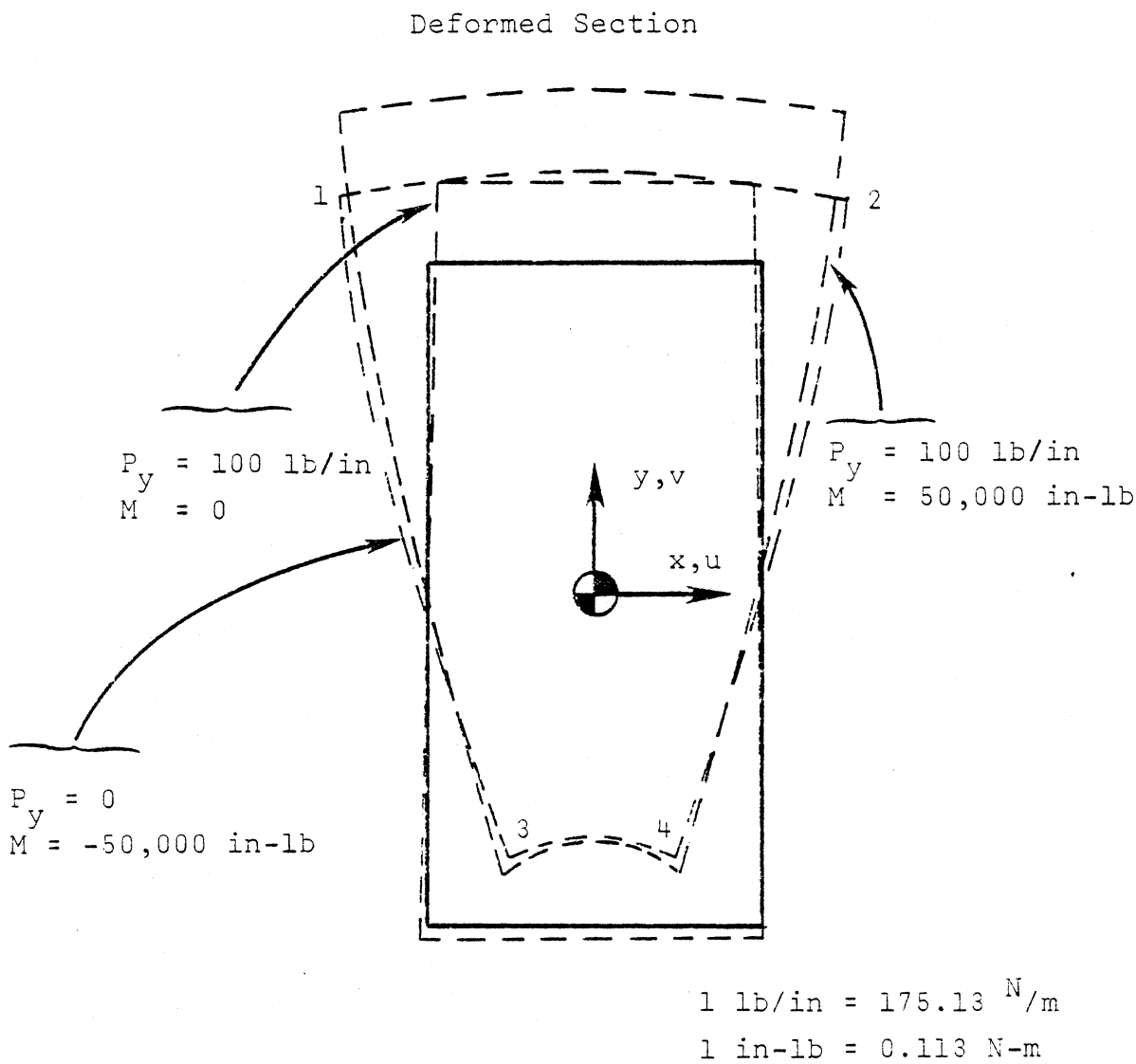

Figure 9. The cross-sectional distortion of a solid rectangular section due to three different loading conditions.

Circular Section

Next, consider a homogeneous beam with a solid circular cross section in which the material has a modulus of elasticity of 199,950 MPa (29,000,000 psi) and a Poisson's ratio of 0.27. Figure 10 depicts the finite element idealization with the circular boundary of the cross section modeled as a series of straight lines.

The beam is loaded by a shearing force in the x direction of 444.82 N (100 lb.) and a body force of 0.273×10^{-3} N/mm^3 (1 lb./in.^{3}) in the x direction. The exact solution for this problem is given by Love[9] and comparisons of exact and finite element stresses for a quarter of the cross section are presented in Tables 2 and 3. These tables illustrate that the normal stresses from the finite element model compare reasonably well with the exact solutions while the finite element shearing stresses compare very well with the exact ones.

To obtain displacements, nodes 26 and 44 were restrained in the x direction while node 35 was restrained in the y direction. The resulting distortion of the cross section is shown in Figure 11.

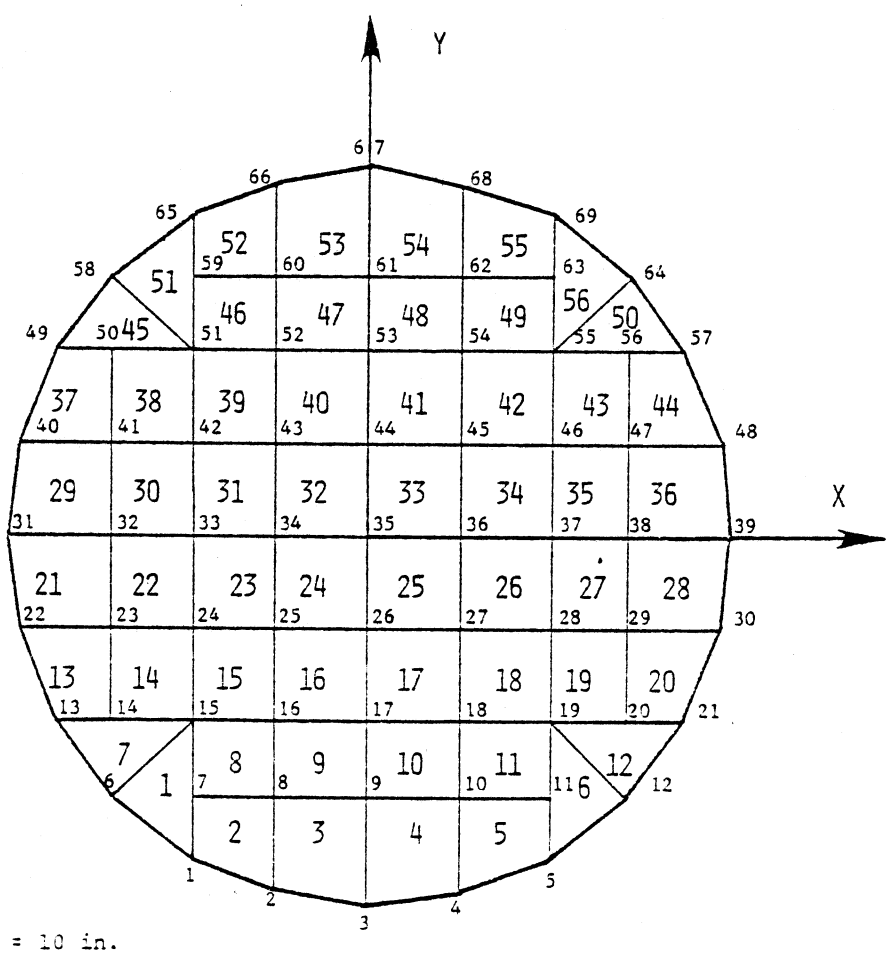

R = 10 in.
(1 in. = 25.4 mm)

Figure 10. The finite element representation of a solid circular section.

TABLE 2

Comparison of Normal Stresses For a Circular Section

Element Number	σ_x		σ_y		σ_z	
	Exact*	F. E.**	Exact*	F. E.**	Exact*	F. E.**
1	-1.1537	-1.046	-0.8139	-0.7309	-0.5441	-0.5875
2	-0.9544	-0.8781	-0.3762	-0.3353	-0.4249	-0.4991
3	-0.3789	-0.3502	-0.1115	-0.0868	-0.0620	-0.0753
7	-1.1144	-0.9415	-1.3642	-1.166	-0.6854	-0.6830
8	-1.0555	-0.9540	-0.7147	-0.6041	0.5731	0.5621
9	-0.4199	-0.3847	-0.2487	-0.2302	0.3426	0.3301
13	-0.9014	-0.7187	-1.9447	-1.797	-0.9088	-0.9722
14	-1.3161	-1.126	-1.4999	-1.354	0.9116	0.9511
15	-1.1312	-1.050	-0.9681	-0.9028	1.3202	1.339
16	-0.4457	-0.4086	-0.3352	-0.3022	0.5974	0.6019
21	-0.8655	-0.5855	-2.3367	-2.125	-0.4048	-0.4042
22	-1.3856	-1.269	-1.7327	-1.614	1.5978	1.653
23	-1.1749	-1.072	-1.1144	-1.026	1.7515	1.784
24	-0.4606	-0.4238	-0.3851	-0.3558	0.7445	0.7532

* Exact solutions from Love in psi
** Finite element solutions in psi

1 psi = 6.89 kPa

TABLE 3

Comparison of Shear Stresses For a Circular Section

Element Number	τ_{xy}		τ_{xz}		τ_{yz}	
	Exact*	F. E.**	Exact*	F. E.**	Exact*	F. E.**
1	0.5331	0.5549	0.2807	0.2748	-0.1480	-0.1459
2	0.2705	0.2737	0.3418	0.3407	-0.1188	-0.1175
3	-0.0300	-0.0157	0.3950	0.3955	-0.0422	-0.0419
7	0.6923	0.7310	0.2118	0.2120	-0.1480	-0.1496
8	0.1476	0.1832	0.3588	0.3595	-0 0884	-0.0952
9	-0.0852	-0.0749	0.4152	0.4171	-0.0302	-0.0312
13	0.6595	0.6363	0.1432	0.1388	-0.1188	-0.1183
14	0.3210	0.3541	0.2737	0.2679	-0.0884	-0.0927
15	0.0675	0.0662	0.3715	0.3741	-0.0556	-0.0559
16	-0.0788	-0.0697	0.4279	0.4302	-0.0190	-0.0196
21	0.2417	0.2280	0.1259	0.1222	-0.0422	-0.0416
22	0.1045	0.1122	0.2811	0.2816	-0.0315	-0.0323
23	0.0181	0.0256	0.3788	0.3802	-0.0190	-0.0197
24	-0.0318	-0.0297	0.4352	0.4376	-0.0065	-0.0066

* Exact solutions from Love in psi
** Finite element solutions in psi

1 psi = 6.89 kPa

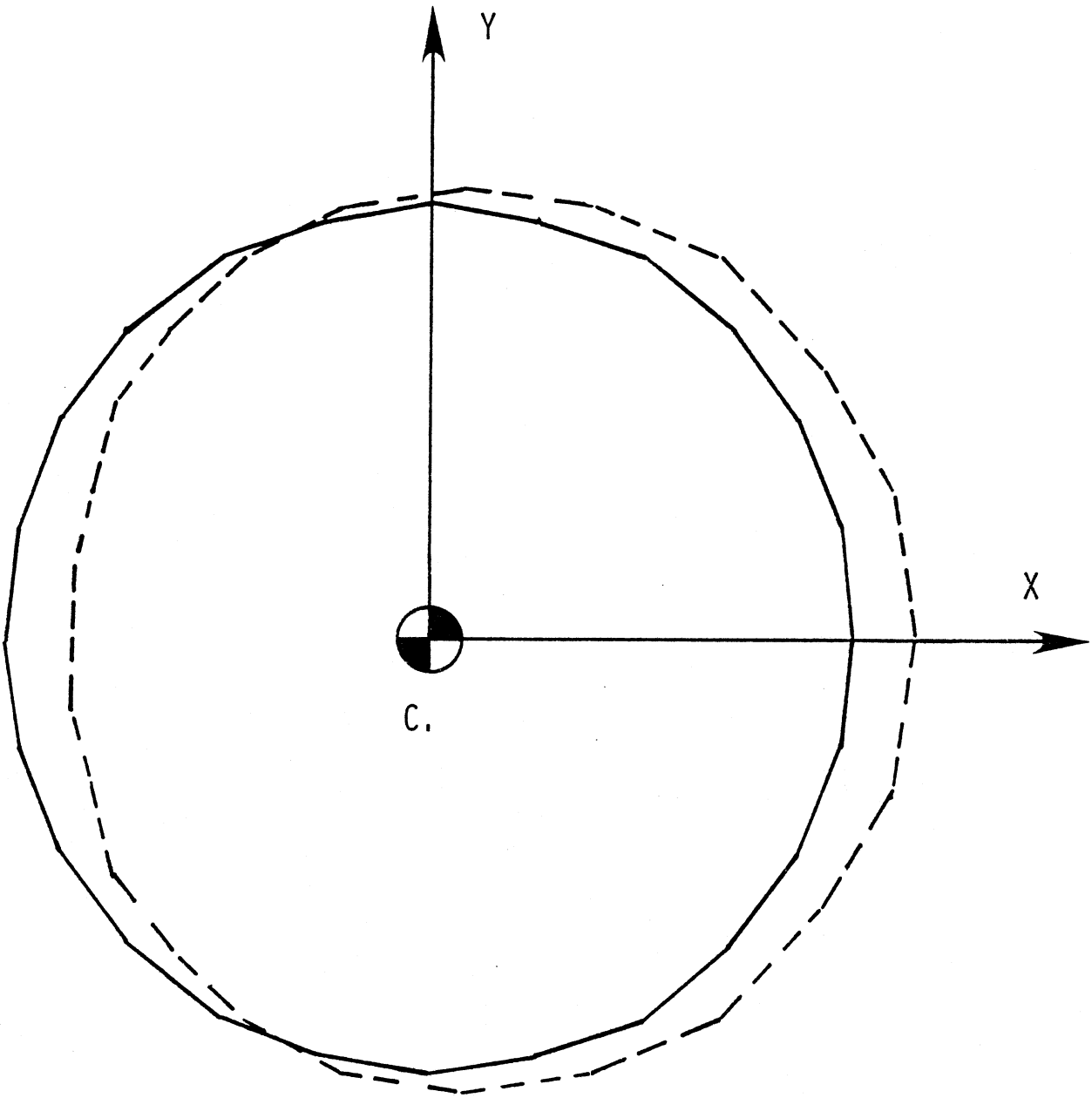

Figure 11. The cross-sectional distortion of a solid circular section due to an x body force of 1 lb./in.^{3}

$1\ ^{lb}/in^3 = 0.273 \times 10^{-3}\ ^{N}/mm^3$

Zee Section

To demonstrate that the numerical procedure described in this study is equivalent to previous studies which consider only nonuniform torsion, a zee section, depicted in Figure 12, was analyzed. This section is identical to the one studied by Perrone and Pilkey.[13] The beam has a modulus of elasticity of 199,950 MPa (29,000,000 psi) and a Poisson's ratio of 0.27 and is subjected to a bimoment of $-686.04\ N\cdot m^2$ ($-239,055$ lb.-in.^{2}).

Since input into the present finite element formulation considers only the rate of change of twisting moment, some modification must be made to consider bimoments due to restrained torsion. It may be shown[7] that

$$B_\phi = E\Gamma_\phi \alpha'', \tag{35}$$

where

$$\alpha'' = -\frac{1}{GJ}\Omega . \tag{36}$$

Since the term of interest is α'', eq. (35) may be solved for α'' in terms of the bimoment and substituted in eq. (36) to give the rate of change of twisting moment or the twisting moment per unit length about the shear center in terms of the bimoment.

$$\Omega = -\frac{JB_\phi}{2(1+\mu)\Gamma_\phi} . \tag{37}$$

It should be emphasized that eq. (37) gives the twisting moment per unit length about the shear center, while the finite element formulation considers only twisting moments about the centroid. If the shear center and centroid do not coincide, then the twisting moment per unit length given by eq. (37) must be computed about the centroid by statics.

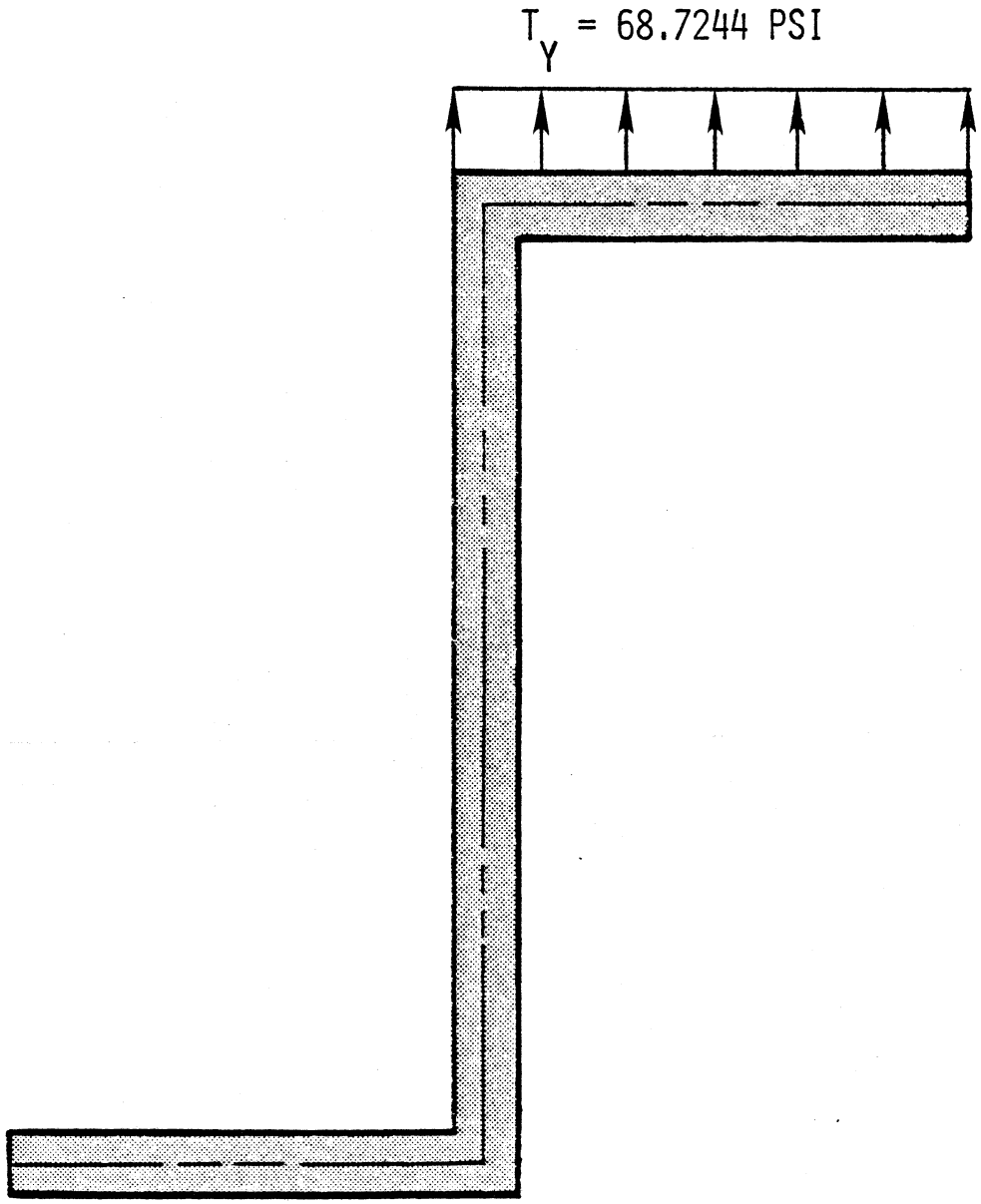

1 psi = 6.89 kPa

Figure 12. Surface tractions on a zee section corresponding to a bimoment force.

Using the values given by Perrone and Pilkey of $J = 327.35 \times 10^3$ mm^4 (78.64583×10^{-2} $in.^4$) and $\overline{\phi} = 41.32 \times 10^9$ mm^6 (153.8617 $in.^6$), eq. (37) gives a value of $\Omega = 2140$ N·m/m. (481.07 in.-lb./in.). Table 4 gives the values of the normal stress due to restrained torsion on the upper flange of the zee section, which are identical to the results obtained by Perrone and Pilkey. These normal stresses do not contain the contribution due to the plane strain solution. To obtain the plane strain solution, it is necessary to induce surface tractions on the cross section that will produce a twisting moment per unit length about the centroid corresponding to Ω. The manner in which these surface tractions are applied is completely arbitrary and, in this case, a surface traction of 473.84 kPa (68.7244 psi) in the y direction distributed uniformly as depicted in Figure 12 will give a twisting moment per unit length of 2140 n.-m/m (481.07 in.-lb./in.) about the centroid of the section.

Table 5 gives the additional normal stresses on the upper flange due to the plane strain problem. These additional stresses are significantly smaller in comparison to those due to restrained torsion and may be neglected. However, the plane strain solution will give the cross-sectional distortion of the cross section as depicted in Figure 13. For the plane strain solution, node 25 was pinned and node 32 was restrained in the y direction.

This example demonstrates that the finite element method will give equivalent results to other formulations for restrained torsion.

TABLE 4

Normal Stresses on a Zee Section
Due to Restrained Torsion

Element Number	σ_z (psi)
1	-1.48896E+04
2	-1.19764E+04
3	-9.06325E+03
4	-6.15006E+03
5	-3.23688E+03
6	-3.23688E+02
7	2.58950E+03
8	5.43795E+03

1 psi = 6.89 kPa

TABLE 5

The Additional Normal Stress on a Zee Section Due to the Plane Strain Solution

Element Number	σ_z (psi)
1	-10.45
2	13.24.
3	11.13
4	12.18
5	16.83
6	-11.05
7	176.90
8	-165.80

1 psi = 6.89 kPa

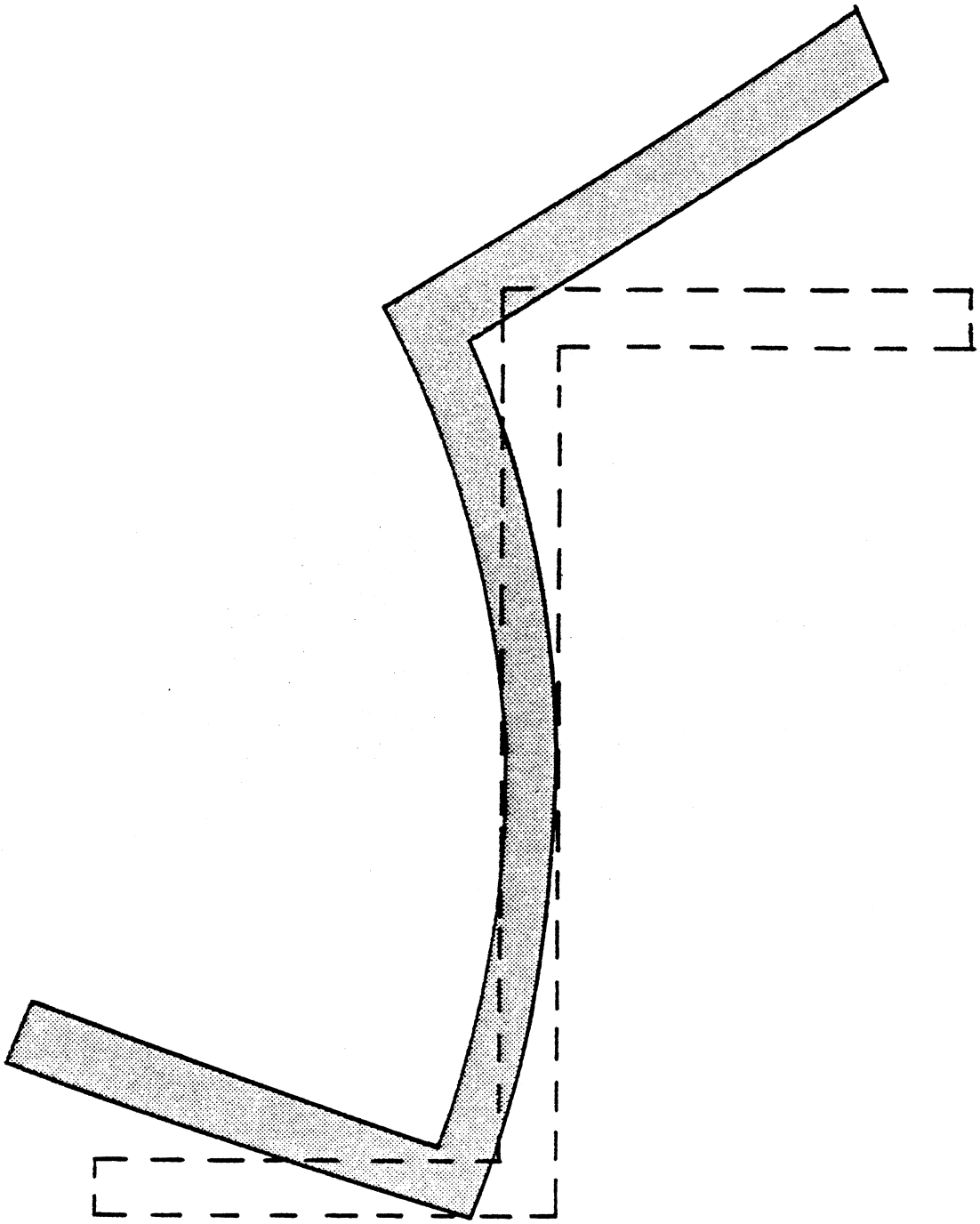

Figure 13. The cross-sectional distortion of a zee section.

Box Section

Consider a homogeneous beam of a thin walled box cross section that has a modulus of elasticity of 199,950 MPa (29,000,000 psi) and a Poisson's ratio of 0.27. Figure 14 depicts the dimensions and the finite element idealization of the cross section. Loading on the box section consists of a rate of change of shear in the y direction of 17,512.7 N/m (100 lb./in.) uniformly distributed on the upper surface of the section as a surface traction of 68.95 kPa. Since the surface tractions are symmetrical with respect to the centroid of the section, there are no induced stresses due to nonuniform torsion.

A plot of the normal stress induced by the nonuniform shear is shown in Figure 15, which shows that the upper corners of the box are more highly stressed than the remainder of the cross section.

The plane strain solution can again be used to obtain the cross-sectional distortion of the cross section to within a rigid body mode. A plot of the cross-sectional distortion for the case where node 5 is pinned and node 14 restrained in the x direction is depicted in Figure 16. The choice of the boundary condition in determining the u and v displacements has no effect on the derived stresses.

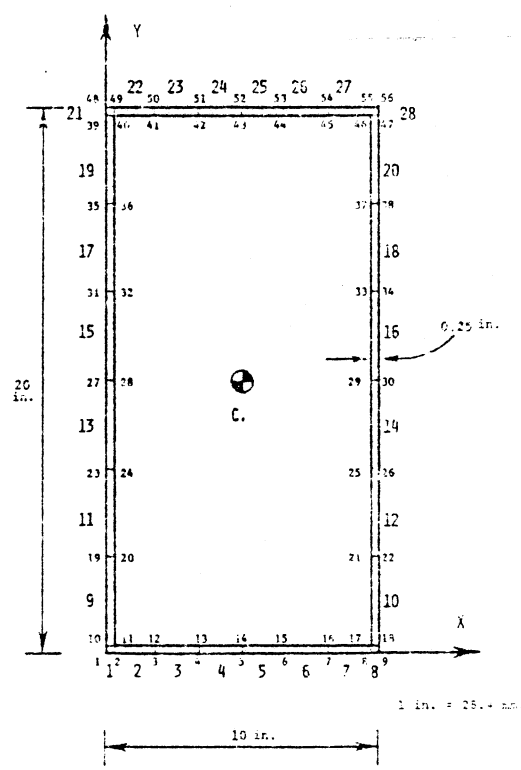

Figure 14. Dimensions and the finite element representation of a rectangular box section.

2022

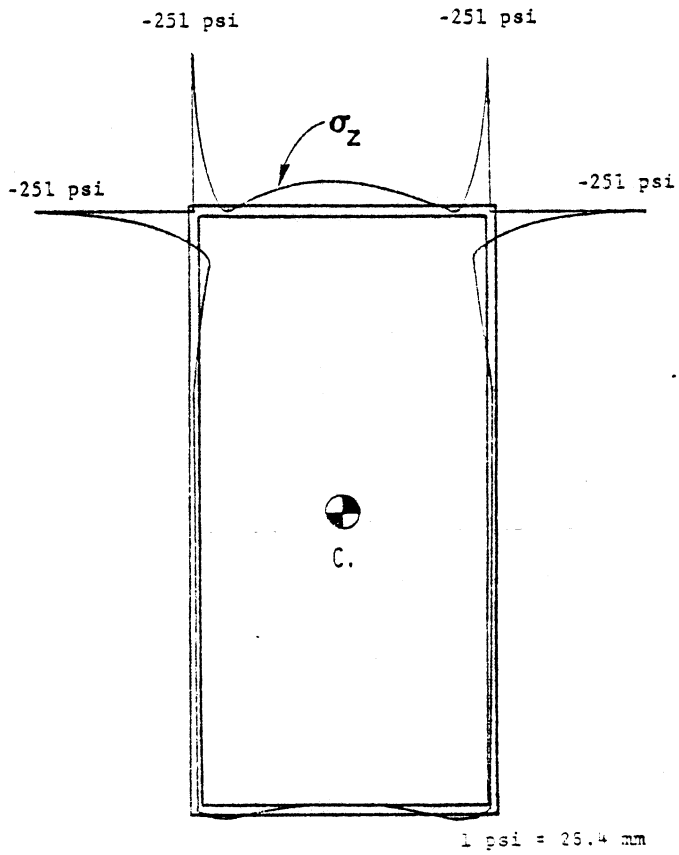

Figure 15. The normal stress (σ_z) distribution in a box section due to nonuniform shear.

2025

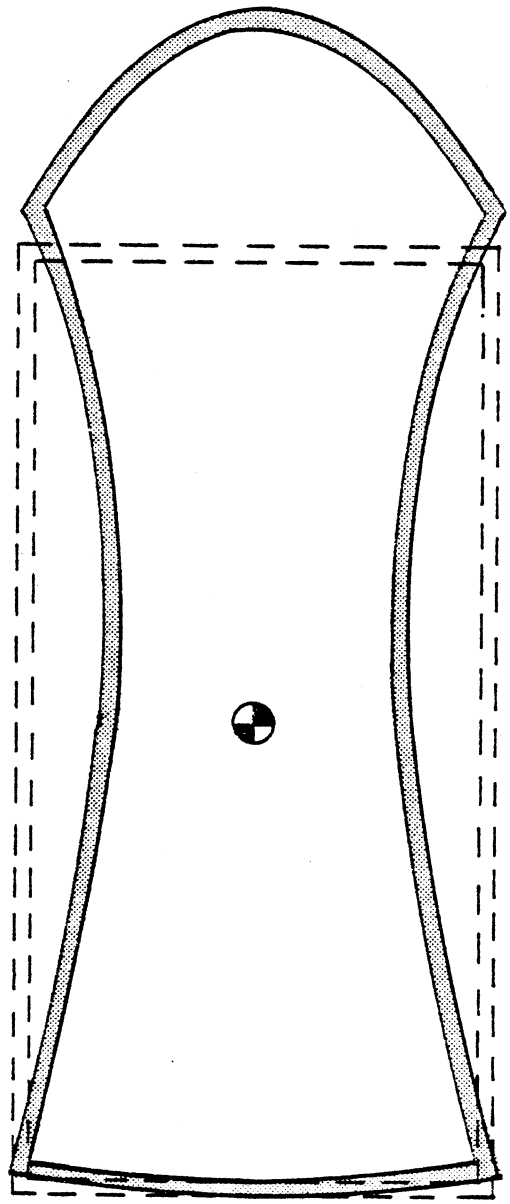

Figure 16. The cross-sectional distortion of a box section.

Channel Section

Consider a homogeneous beam consisting of a thin walled channel section which has a modulus of elasticity of 199,950 MPa (29,000,000 psi) and a Poisson's ratio of 0.27. Figure 17 depicts the dimensions and the finite element idealization of the cross section. Loading on the channel section consists of a rate of change of shear in the y direction of 17,512.7 N/m (100 lb./in.) uniformly distributed on the upper flange of the channel as a surface traction of 172.37 kPa (25 psi). Since the surface tractions are not symmetrical with respect to the centroid, there will be a rate of change of twisting moment about the centroid of -363.27 N-m/m (-81.667 in.-lb./in.) that will induce nonuniform torsional stresses.

Figure 18 is a plot of the longitudinal normal stresses induced on the channel section by the system of forces just described. It is interesting to note that the normal stresses through the flanges vary in a nearly linear fashion. The dashes in the plot near the ends of the flanges indicate no available data at those end points and that extrapolation was used.

To obtain the cross-sectional distortion of the cross section, node 40 in Figure 17 was pinned and the vertical displacement of node 25 was restrained. The resulting distortion of the channel section is shown by Figure 19.

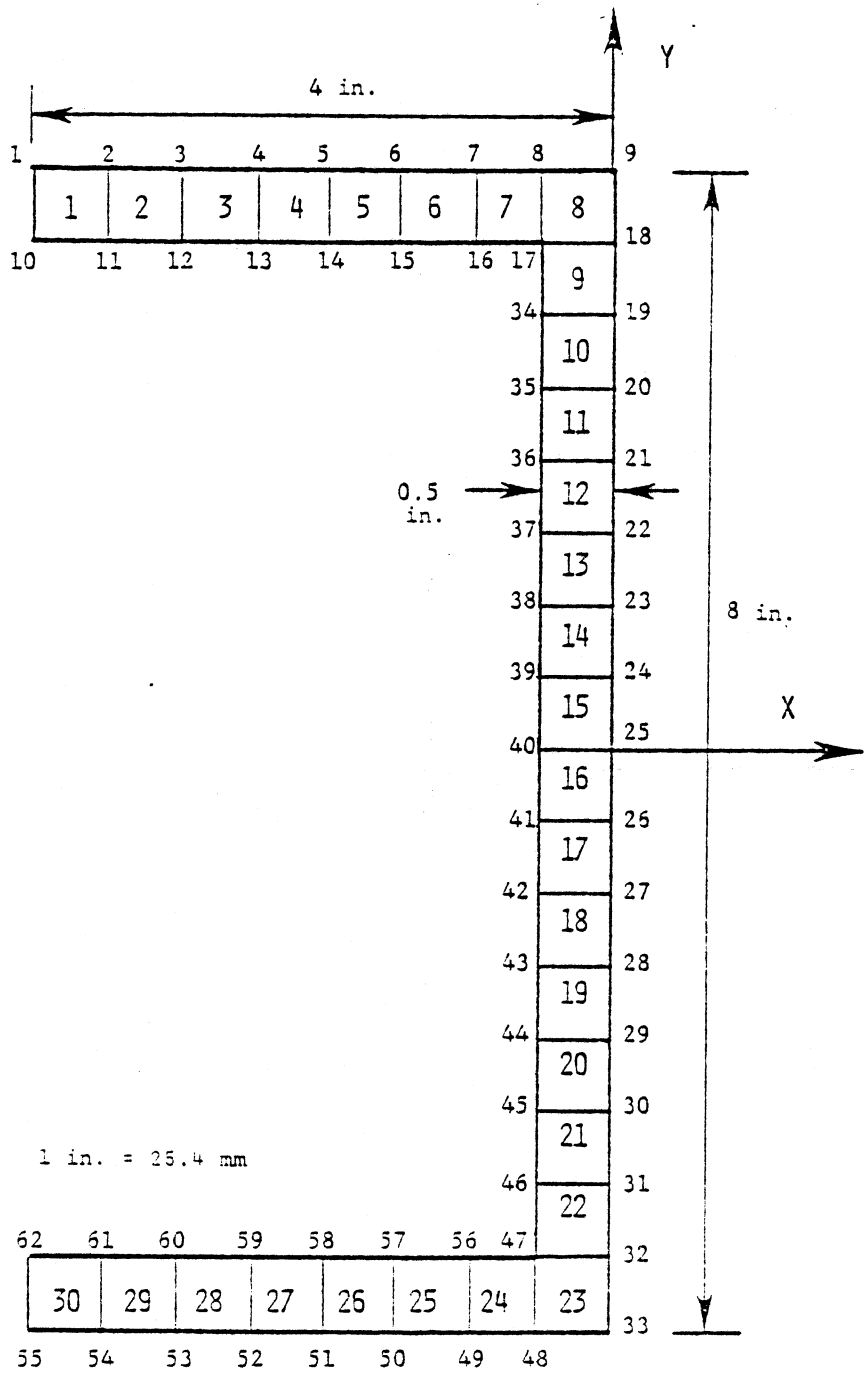

Figure 17. Dimensions and the finite element representation of a channel section.

2025

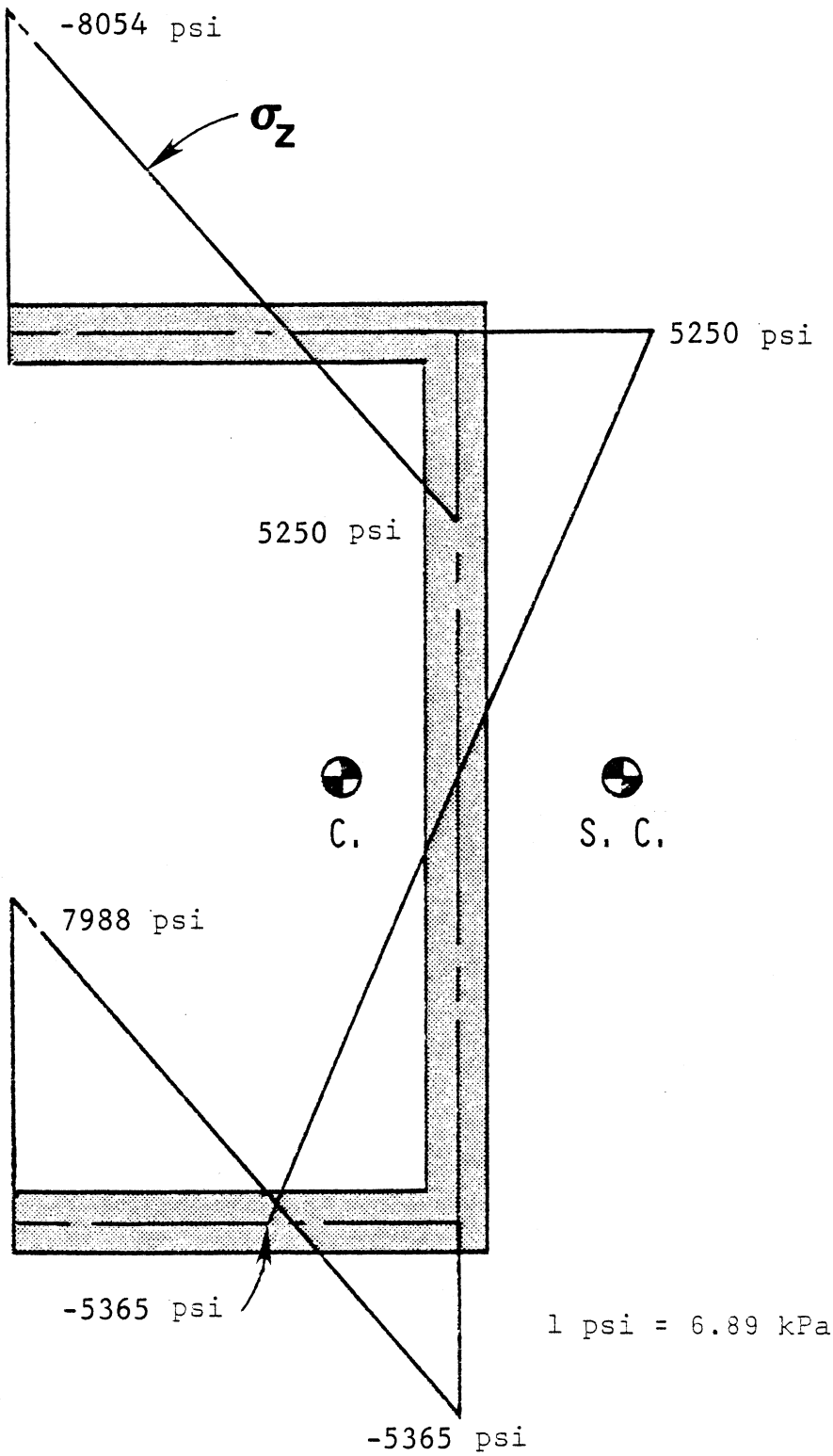

Figure 18. The normal stress (σ_z) distribution in a channel section due to nonuniform shear and torsion.

2027

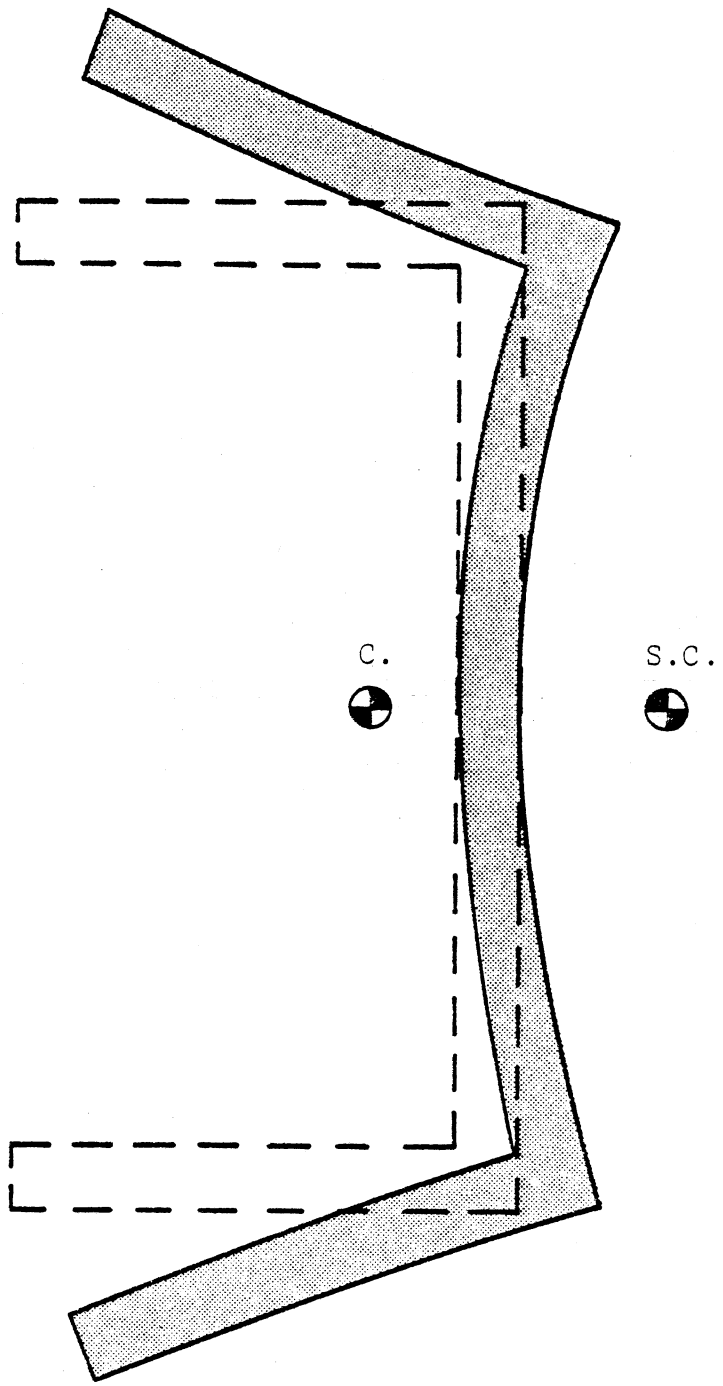

Figure 19. The cross-sectional distortion of a channel section.

DISCUSSION OF RESULTS

The finite element stresses compared extremely well with the generalized plane stress solution for the rectangular section. Considering that the boundary of the solid circular section was approximated by a series of straight-line segments, these finite element stresses also compared very favorably with the exact ones. The zee section problem demonstrated that this methodology yields equivalent results to other formulations whenever nonuniform torsion is considered.

The box section problem demonstrated that the plane strain solution yields the cross-sectional distortion within a rigid body mode. Both the box and the channel section problems indicate the application of the present formulation to common bridge cross sections.

SUMMARY AND CONCLUSIONS

Summary

The theoretical background, formulation, and methodology were developed for the elastic stress analysis of general prismatic beams. The applied forces included axial force, bending moment, uniform torsion, constant shear, and the rates of change of twisting moment, axial force, and shear. By making certain assumptions, the formulation expressed in terms of displacement functions was reduced from a three-dimensional analysis to a two-dimensional one. Numerical solutions were obtained using the finite element method, and the results were compared with either the exact or approximate solutions for beams having certain cross-sectional shapes. The solutions to several problems having commonly used bridge cross-sectional shapes were given to demonstrate the applicability of this methodology.

Conclusions

The comparisons between the numerical solutions obtained by the finite element analysis and the exact solutions for beams of certain cross sections agreed favorably and tended to validate the reliability of the solution technique used. The ability to analyze beams having commonly used bridge shapes demonstrated the applicability of this method.

Whenever the stress resultants are known, the formulations derived in this study would enable a designer to determine more accurately than conventional methods of analyses the stresses on a

particular cross section of a bridge. Since designers draw shear, moment, torque, thrust, and loading diagrams for a bridge, the particular stress resultants emphasized in this study — the rates of change of torque, shear, and axial force — may be determined simply by taking the slopes of the these diagrams at a particular section along the bridge.

It is difficult to determine under what conditions the normal stresses resulting from nonuniform shear or torsion may be significant in comparison to bending stresses. This difficulty may be attributed to the fact that the normal stresses due to bending are functions of only the moments while the stresses obtained from nonuniform shear and torsion are functions of entirely different functions (rates of change of shear and torsion).

In addition to obtaining stresses, the method developed in this study predicts the cross-sectional distortion of a beam to within a rigid body mode. The in-plane displacements obtained from the finite element analysis for a solid rectangular section under pure bending compared favorably with exact solutions.

Results from this study should provide designers with valuable information regarding additional normal stresses imposed by non-uniform loading and the deformed shape of beam cross sections.

REFERENCES

1. Vlasov, V. S., Thin-Walled Elastic Beams, National Science Foundation, Washington, D. C., 1961.

2. Heins, C. P., Bending and Torsional Design in Structural Members, D. C. Heath and Company, Lexington, Mass., 1975.

3. Krahula, J. L., "Analysis of Bent and Twisted Bars Using the Finite Element Method, AIAA Journal, Vol. 5, No. 6, June,1967, pp. 1194-1197.

4. Chang, P. Y., Thasanatorn, C., and Pilkey, W. D., "Restrained Warping Stresses in Thin-Walled Open Sections", ASCE, Structural Division Journal, Vol. 10, ST11, Nov., 1975, pp. 2467-2472.

5. Mason, W. E., Jr., and Herrmann, L. R., "Elastic Shear Analysis of General Prismatic Beams", ASCE, Engineering Mechanics Division, August, 1968, pp. 965-983.

6. Herrmann, L. R., "Elastic Torsional Analysis of Irregular Shapes", ASCE, Engineering Mechanics Division, December, 1965, pp. 11-19.

7. Leftwich, S. D., Elastic Stress Analysis of General Prismatic Beams, Doctoral Dissertation, School of Engineering and Applied Science, University of Virginia, Charlottesville, Virginia, 1980.

8. The Structural Members Users Group, Technical Manual, a supplement to the McGraw-Hill book Modern Formulas for Statics and Dynamics, W. D. Pilkey and P. Y. Chang, 1978.

9. Love, A. E. H., A Treatise on the Mathematical Theory of Elasticity, 4th ed., Dover Publications, New York, 1944.

10. Sokolnikoff, I. S., Mathematical Theory of Elasticity, 2nd ed., McGraw-Hill Book Company, Inc., New York, 1956.

11. Boresi, A. P., and Lynn, P. P., Elasticity in Engineering Mechanics, Prentice-Hall, Inc., Englewood Cliffs, New Jersey, 1974.

12. Timoshenko, S. P., and Goodier, J. N., Theory of Elasticity, 3rd ed., McGraw-Hill Book Company, Inc., New York, 1970.

13. Structural Mechanics Software Series, Vol. I, edited by N. Perrone and W. Pilkey, University Press of Virginia, Charlottesville, Virginia, 1977, pp. 413-417.

2032